

Analytical approach to the two-site Bose-Hubbard model: from Fock states to Schrödinger cat states and entanglement entropy

Luca Dell'Anna

*Dipartimento di Fisica e Astronomia "Galileo Galilei",
Università di Padova, via F. Marzolo 8, 35131 Padova, Italy*

Abstract

We study the interpolation from occupation number Fock states to Schrödinger cat states on systems modeled by two-mode Bose-Hubbard Hamiltonian, like, for instance, bosons in a double well or superconducting Cooper pair boxes. In the repulsive interaction regime, by a simplified single particle description, we calculate analytically energy, number fluctuations, stability under coupling to a heat bath, entanglement entropy and Fisher information, all in terms of hypergeometric polynomials of the single particle overlap parameter. Our approach allows us to find how those quantities scale with the number of bosons. In the attractive interaction regime we calculate the same physical quantities in terms of the imbalance parameter, and find that the spontaneous symmetry breaking, occurring at interaction U_c , predicted by a semiclassical approximation, is valid only in the limit of infinite number of bosons. For a large but finite number, we determine a characteristic strength of interaction, U_c^* , which can be promoted as the crossover point from coherent to incoherent regimes and can be identified as the threshold of fragility of the cat state. Moreover, we find that the Fisher information is always in direct ratio to the variance of on-site number of bosons, for both positive and negative interactions. We finally show that the entanglement entropy is maximum close to U_c^* and exceeds its coherent value within the whole range of interaction between $2U_c$ and zero.

I. INTRODUCTION

The two-mode Bose-Hubbard model is commonly used to describe several systems like, for examples, the bosonic double well traps [1–6] or the superconducting Cooper pair boxes [7, 8, 11–13]. It has been recently used as the building block for studying spinful bosonic systems on double-well lattices [14]. In spite of its simplicity, being an interacting problem, although integrable [15] and whose low energy spectrum was explored in the weak interaction regime [16], it is far from a simple solution for a generic number of bosons and interaction strength. Because of that reason, usually one resorts to numerical approaches which are simple and very efficient, giving up trying to describe the system analytically, although not exactly. A first issue worth being addressed is, therefore, that of providing a simple description which allows one to find handy and analytical expressions for several physical quantities and their scalings with the number of bosons. In order to discriminate between the so-called quantum phase model [9], expressed by occupation number states, and the mean field model [10], formulated in terms of coherent states, emerging from the solution of the classical Gross-Pitaevski equation - both models invoked to describe, for instance, the charge oscillations in the superconducting Cooper pair boxes - it can be useful to study certain stability properties [11]. The two models, in fact, behave quite differently in the presence of noise induced by a weakly coupled external environment, therefore it is crucial to predict how the relaxation time scales with the number of bosons.

In this paper we propose, therefore, to tackle the problem of describing the ground state of a two-mode Bose-Hubbard model from an intuitive and physically transparent description, although approximate. Our proposal is based on the observation that the norm of a Fock state, which is the ground state for strongly repulsive interacting bosons, $|\psi_F\rangle = (a_L^\dagger)^n (a_R^\dagger)^k |0\rangle$, (where $a_{L,R}^\dagger$ are creation operators on left, L , or right, R , site) is given by the permanent (Per) of a diagonal block overlap matrix

$$\langle\psi_F|\psi_F\rangle = \text{Per} \left(\begin{array}{c|c} 1_{n\times n} & 0_{n\times k} \\ \hline 0_{k\times n} & 1_{k\times k} \end{array} \right),$$

where, schematically, the blocks denoted by “1” are made of all elements equal to one and the blocks denoted by “0” are made of all null elements. On the other hand, the norm of a coherent-like state, or sometimes called phase state, ground state for free bosons, $|\psi_C\rangle = (\xi_L a_L^\dagger + \xi_R a_R^\dagger)^{n+k} |0\rangle$, with $|\xi_L|^2 + |\xi_R|^2 = 1$, is given by the permanent of a fully constant matrix

$$\langle\psi_C|\psi_C\rangle = \text{Per} \left(\begin{array}{c|c} 1_{n\times n} & 1_{n\times k} \\ \hline 1_{k\times n} & 1_{k\times k} \end{array} \right).$$

A natural expectation is, therefore, that, going from number Fock state to fully delocalized coherent-like state, the bosons, initially localized on the two sites, start to overlap, making finite the off-diagonal blocks of the overlap matrix. Our ansatz is that the intermediate interaction regime can be fairly described by the state $|\psi\rangle$, written in Eq. (9), that describes

two condensates which can be localized on each site in the Fock limit while merging together in the coherent one, and whose norm is given by

$$\langle \psi | \psi \rangle = \text{Per} \left(\begin{array}{c|c} 1_{n \times n} & \omega_{n \times k}^* \\ \hline \omega_{k \times n} & 1_{k \times k} \end{array} \right),$$

where ω is indeed the overlap of the single particle wavefunctions, as we will be seeing. In the site-symmetric case, then, this description allows us to interpolate from Fock to coherent-like states by varying a single parameter, ω , which has a clear physical meaning and can be fixed variationally in terms of the number of bosons and the microscopic parameters of the Hubbard model.

Another important issue is related to the spontaneous symmetry breaking between the two wells, which is supposed to occur in the attractive interaction regime. The experimental realization of a double-well potential which confines ultracold alkali-metal atoms, is the atomic analog of the superconducting Josephson junction [17–20], as predicted several years ago [21]. The Josephson equations are valid in the weak interaction regime and predicts self-trapping and symmetry breaking of the atomic population in the two wells [22–25]. The symmetry breaking can be derived starting from quasiclassical coherent states. We will consider, instead, coherent-like states, i.e. $|\psi_C\rangle$, given by the contributions to the full coherent states with fixed number of particles, which is the case in real experimental situations. Also these states exhibit a symmetry breaking, however we show that a symmetric linear combination of two of such states, namely a macroscopic Schrödinger-cat state [4, 26, 27], which has null population imbalance, is energetically favoured, for equal local energies. As a result, in the case of fixed number of particles, the symmetry breaking should not occur and the imbalance parameter, which does not correspond to the population imbalance, is finite for any attractive interaction. This result is in agreement also with numerical results [28], and, at some extent, consistent with the semiclassical approach in the limit $N \rightarrow \infty$. We find, however, a discontinuity in the imbalance parameter at some critical strength of interaction. This is a spurious effect of our ansatz for the ground state, however it reveals the fragility of the cat state below a certain value of the interaction. Nevertheless, by numerical checks, we observed that, around that value of interaction, some physical quantities have large derivatives and the energy changes its behavior. At that point the coherence visibility drops while the cat state becomes extremely fragile. The relaxation time, in fact, goes like $1/N^2$ upon an asymmetric coupling with an external bath. One can identify such a threshold as the critical interaction below which an infinitesimally small mismatch between the two on-site energies can produce a macroscopic population imbalance.

Finally we investigate the behavior of the entanglement entropy and the Fisher information. The quantum entanglement applied to many body systems has attracted a lot of theoretical interest in recent years (see, for instance, Refs. [29, 30] and references therein). One would expect that the entanglement entropy reaches its maximum in the presence of large coherence. We show, instead, that, in agreement with numerical results [28], the max-

imum entropy occurs close to the putative symmetry breaking point. In particular we found that the entropy exceeds its value obtained in the case of free bosons, in a whole range of attractive interaction which goes from zero to twice the critical interaction of the symmetry breaking. We finally show that, for almost all the range of interaction, i.e. $-\infty < U \ll N$, the Fisher information F is always directly proportional to the variance of on-site number of bosons σ , as described by the equation $F = 4\sigma/N^2$.

The paper is organized as follows. In Sec. II we introduce some useful definitions; in Sec. III we present the model and our ansatz for the approximate ground state in the repulsive interaction regime; in Sec. IV we perform detailed calculations for generic two and four-point correlation functions, useful to calculate several quantities of interest; in Sec. V and VI we recover the exact results, respectively, for strongly repulsive interacting and free bosons; in Sec. VII we derive asymptotic behaviors in the large N limit for energy, decay rate, number fluctuations and coherent visibility; in Sec. VIII we calculate, by our ansatz for repulsive interaction ground state, the entanglement entropy and the Fisher information. Section IX, instead, is devoted to the analysis of attractive interaction, calculating all the quantities of interest as Schrödinger cat state mean values and finally in Sec. X we derive entanglement entropy and Fisher information, always in the attractive regime. We summarize the main results showing some plots in Sec. XI, and drawing some conclusions in the final section.

II. GENERAL REMARKS

Let us first consider N bosons on a lattice with N_s sites and take the following, not normalized, many-body wavefunctions

$$|\psi\rangle = \prod_{\alpha=1}^N \left(\sum_{i=1}^{N_s} \xi_{\alpha i} a_i^\dagger \right) |0\rangle, \quad (1)$$

$$|\varphi\rangle = \prod_{\alpha=1}^N \left(\sum_{i=1}^{N_s} \eta_{\alpha i} a_i^\dagger \right) |0\rangle. \quad (2)$$

where $\xi_{\alpha i}$ and $\eta_{\alpha i}$ are single particle wavefunctions. It has been shown that such states are rich enough to exhibit both superfluid and insulating behaviors [31]. After defining the $N \times N$ matrix

$$\Omega_{\alpha\beta} = \sum_i \eta_{\alpha i} \xi_{\beta i}^*, \quad (3)$$

the $(N+1) \times (N+1)$ matrix

$$D_{ij} = \begin{pmatrix} \hat{\Omega} & \hat{\eta}_i \\ \hat{\xi}_j^\dagger & \delta_{ij} \end{pmatrix}, \quad (4)$$

and the $(N + 2) \times (N + 2)$ matrix

$$I_{lijm} = \begin{pmatrix} \hat{\Omega} & \hat{\eta}_i & \hat{\eta}_l \\ \hat{\xi}_j^\dagger & \delta_{ij} & \delta_{il} \\ \hat{\xi}_m^\dagger & \delta_{im} & \delta_{ml} \end{pmatrix}, \quad (5)$$

where $\hat{\eta}_i$ is an N -vector with components $\eta_{\alpha i}$, we get the following relations [31]

$$\langle \psi | \varphi \rangle = \text{Per}(\Omega), \quad (6)$$

$$\langle \psi | a_i a_m^\dagger | \varphi \rangle = \text{Per}(D_{lm}), \quad (7)$$

$$\langle \psi | a_i a_i a_j^\dagger a_m^\dagger | \varphi \rangle = \text{Per}(I_{lijm}), \quad (8)$$

where $\text{Per}(A)$ is the permanent of the matrix A . Quite in general, since the calculus of permanents is not easy, it is hard to find handy and analytical expressions for the correlation functions.

III. THE INTERPOLATING STATE

Now let us take $N = n + k$ bosons on two sites, like in a double well, and consider the following many-body state

$$|\psi\rangle = \left(\xi_{1L} a_L^\dagger + \xi_{1R} a_R^\dagger \right)^n \left(\xi_{2L} a_L^\dagger + \xi_{2R} a_R^\dagger \right)^k |0\rangle \quad (9)$$

which is a simplified version of the permanent in Eq. (1), where $\forall \alpha$ such that $\alpha \leq n$, $\xi_{\alpha i} = \xi_{1i}$ while $\forall \alpha$ such that $n < \alpha \leq (n + k)$, $\xi_{\alpha i} = \xi_{2i}$. Defining the unit $n \times k$ matrix (with n rows and k columns) with all elements equal to 1,

$$J^{(n,k)} = \begin{pmatrix} 1 & 1 & \dots & 1 \\ \vdots & \vdots & \dots & \vdots \\ 1 & 1 & \dots & 1 \end{pmatrix}, \quad (10)$$

we can construct the overlap matrix

$$\Omega^{n,k} = \begin{pmatrix} bJ^{(n,n)} & \omega^* J^{(n,k)} \\ \omega J^{(k,n)} & bJ^{(k,k)} \end{pmatrix}, \quad (11)$$

where

$$b = |\xi_{1L}|^2 + |\xi_{1R}|^2 = |\xi_{2L}|^2 + |\xi_{2R}|^2 \quad (12)$$

is the normalization of the single particle wavefunction, therefore we can set $b = 1$. However, for the moment, in order to derive more general relations, we will keep the writing b . The other parameter is

$$\omega = \xi_{2L} \xi_{1L}^* + \xi_{2R} \xi_{1R}^* \quad (13)$$

which is, therefore, the single particle overlap term. For normalized single particle wavefunctions, namely when $b = 1$, we have $0 \leq |\omega| \leq 1$.

Eq. (9) is the simplest permanent state which interpolates, keeping the same functional form, from number Fock state (when, for instance, $\xi_{1L} = \xi_{2R} = 1$ and $\xi_{2L} = \xi_{1R} = 0$, such that we have n bosons on the left well and k bosons on the right well) to a coherent-like state (when $\xi_{1L} = \xi_{2L}$ and $\xi_{1R} = \xi_{2R}$).

The four parameters, $\xi_{1L}, \xi_{2L}, \xi_{1R}, \xi_{2R}$, are not independent, but linked by the two normalization conditions, Eq. (12). On the contrary Eq. (13) is not a further constraint but leads to a different parametrization, where the overlap coefficient ω replaces one of the ξ -parameters. Moreover, from Eq. (9), one can consider n as another free parameter while k is fixed by $k = N - n$. Therefore, at the end, we have three free state parameters (in general two complex numbers and one integer): ξ_{1L} (one among the four ξ 's), the overlap ω and n .

These values can be related to the parameters of the microscopic model. Let us introduce the Bose-Hubbard model

$$H = -\frac{t}{2} \left(a_L^\dagger a_R + a_R^\dagger a_L \right) + \mu (n_L - n_R) + \frac{U}{2} (n_L(n_L - 1) + n_R(n_R - 1)), \quad (14)$$

where t is the hopping parameter, μ is the difference of local chemical potentials induced for instance by a mismatch between the two wells, and U is the on site interaction. One can therefore link the three parameters ξ_{1L}, ω, n with the three parameters of the Bose-Hubbard model, t, μ, U , by variational analysis. Actually, defining

$$E [\xi_{1L}, n, \omega | t, \mu, U] = \frac{\langle \psi | H | \psi \rangle}{\langle \psi | \psi \rangle}, \quad (15)$$

one can partially fix the set of state parameters, requiring that $\delta_{\xi_{1L}} E = \delta_{\omega} E = \delta_n E = 0$, establishing, in this way, a connection between the set of the state parameters with the set of the Hamiltonian ones. The residual arbitrariness can be removed if we require that the amplitudes $\xi_{\alpha i}$ are real.

IV. CORRELATION FUNCTIONS

In order to calculate two and four points correlation functions we have to determine the permanents of the matrices Ω, D and I . As we will see, all these permanents can be calculated analytically. Let us start considering the normalization of the many-body wavefunction Eq. (9). This quantity is given by

$$\langle \psi | \psi \rangle = \text{Per}(\Omega^{n,k}) = n!k! b^{n+k} {}_2F_1 \left(-n, -k, 1; \frac{|\omega|^2}{b^2} \right) \quad (16)$$

which is derived by induction, applying the Laplace theorem for the permanent and where ${}_2F_1(a, b, 1; z)$ is an hypergeometric function. Since the first arguments are integer numbers,

${}_2F_1$ is a polynomial, particularly, using the definition of the Jacobi polynomials $P_n^{(\alpha,\beta)}(z)$, it can be written as follows

$${}_2F_1(-n, -k, 1; z) = P_n^{(0, -n-k-1)}(1-2z). \quad (17)$$

Actually, one can verify that $\text{Per}(\Omega^{n,k})$ satisfies the following recursive equation

$$\text{Per}(\Omega^{n,k}) = n b \text{Per}(\Omega^{n-1,k}) + k! |\omega|^2 b^{k-2} \left[n! b^n + n \sum_{\ell=1}^{k-1} \frac{b^{1-\ell}}{\ell!} \text{Per}(\Omega^{n-1,\ell}) \right] \quad (18)$$

and check that Eq. (16) is a solution. In order to calculate two and four point correlation functions it is convenient to calculate the permanents of the following matrices

$$\mathcal{O}_{1u}^{n,k} = \begin{pmatrix} bJ^{(n-1,n)} & \omega^* J^{(n-1,k-1)} \\ \omega J^{(k,n)} & bJ^{(k,k-1)} \end{pmatrix}, \quad (19)$$

$$\mathcal{O}_{1d}^{n,k} = \begin{pmatrix} bJ^{(n,n-1)} & \omega^* J^{(n,k)} \\ \omega J^{(k-1,n-1)} & bJ^{(k-1,k)} \end{pmatrix}, \quad (20)$$

with dimensions $(n+k-1) \times (n+k-1)$ and

$$\mathcal{O}_{2u}^{n,k} = \begin{pmatrix} bJ^{(n-2,n)} & \omega^* J^{(n-2,k-2)} \\ \omega J^{(k,n)} & bJ^{(k,k-2)} \end{pmatrix}, \quad (21)$$

$$\mathcal{O}_{2d}^{n,k} = \begin{pmatrix} bJ^{(n,n-2)} & \omega^* J^{(n,k)} \\ \omega J^{(k-2,n-2)} & bJ^{(k-2,k)} \end{pmatrix}, \quad (22)$$

with dimensions $(n+k-2) \times (n+k-2)$. Their permanents, together with Eq. (16), are the building blocks useful to construct the permanents of the D -matrix, for the two-point correlation functions, and of the I -matrix, for the four-point correlation functions. By recursion, after several algebraic steps, we get

$$\text{Per}(\mathcal{O}_{1u}^{n,k}) = n!(k-1)! \omega b^{n+k-2} \sum_{\ell=0}^{k-1} {}_2F_1\left(1-n, -\ell, 1; \frac{|\omega|^2}{b^2}\right), \quad (23)$$

$$\text{Per}(\mathcal{O}_{1d}^{n,k}) = (n-1)!k! \omega^* b^{n+k-2} \sum_{\ell=0}^{n-1} {}_2F_1\left(-\ell, 1-k, 1; \frac{|\omega|^2}{b^2}\right), \quad (24)$$

$$\text{Per}(\mathcal{O}_{2u}^{n,k}) = k(n-2)!(k-2)! \omega^2 b^{n+k-4} \sum_{m=0}^{n-2} \left[(1+m) \sum_{\ell=0}^{k-2} {}_2F_1\left(-m, -\ell, 1; \frac{|\omega|^2}{b^2}\right) \right], \quad (25)$$

$$\text{Per}(\mathcal{O}_{2d}^{n,k}) = n(n-2)!(k-2)! \omega^{*2} b^{n+k-4} \sum_{\ell=0}^{k-2} \left[(1+\ell) \sum_{m=0}^{n-2} {}_2F_1\left(-m, -\ell, 1; \frac{|\omega|^2}{b^2}\right) \right]. \quad (26)$$

However we will need only a couple of those permanents since

$$\text{Per}(\mathcal{O}_{1u}^{n,k}) = \text{Per}(\mathcal{O}_{1d}^{n,k})^*, \quad (27)$$

$$\text{Per}(\mathcal{O}_{2u}^{n,k}) = \text{Per}(\mathcal{O}_{2d}^{n,k})^*. \quad (28)$$

We now write the $(n + k + 1) \times (n + k + 1)$ -matrix

$$D_{ij}^{n,k} = \begin{pmatrix} bJ^{(n,n)} & \omega^* J^{(n,k)} & \hat{\xi}_{1i} \\ \omega J^{(k,n)} & bJ^{(k,k)} & \hat{\xi}_{2i} \\ \hat{\xi}_{1j}^\dagger & \hat{\xi}_{2j}^\dagger & \delta_{ij} \end{pmatrix}, \quad (29)$$

where $i, j = L, R$ and with $\hat{\xi}_{1j}^\dagger = \xi_{1j}^*(1, 1, \dots, 1)$, a n -vector and $\hat{\xi}_{2j}^\dagger = \xi_{2j}^*(1, 1, \dots, 1)$, a k -vector. Its permanent, related to two-point correlation functions, can be written as follows

$$\begin{aligned} \langle \psi | a_i a_j^\dagger | \psi \rangle = \text{Per}(D_{ij}^{n,k}) = \delta_{ij} \text{Per}(\Omega^{n,k}) + n \xi_{1i} \left[n \xi_{1j}^* \text{Per}(\Omega^{n-1,k}) + k \xi_{2j}^* \text{Per}(\mathcal{O}_{1u}^{n,k}) \right] \\ + k \xi_{2i} \left[k \xi_{2j}^* \text{Per}(\Omega^{n,k-1}) + n \xi_{1j}^* \text{Per}(\mathcal{O}_{1d}^{n,k}) \right]. \end{aligned} \quad (30)$$

Now defining the $(n + k + 2) \times (n + k + 2)$ matrix

$$I_{lijm}^{n,k} = \begin{pmatrix} bJ^{(n,n)} & \omega^* J^{(n,k)} & \hat{\xi}_{1i} & \hat{\xi}_{1l} \\ \omega J^{(k,n)} & bJ^{(k,k)} & \hat{\xi}_{2i} & \hat{\xi}_{2l} \\ \hat{\xi}_{1j}^\dagger & \hat{\xi}_{2j}^\dagger & \delta_{ij} & \delta_{lj} \\ \hat{\xi}_{1m}^\dagger & \hat{\xi}_{2m}^\dagger & \delta_{im} & \delta_{lm} \end{pmatrix}, \quad (31)$$

with $l, i, j, m = L, R$ we get

$$\begin{aligned} \langle \psi | a_l a_i a_j^\dagger a_m^\dagger | \psi \rangle = \text{Per}(I_{lijm}^{n,k}) \\ = \delta_{lm} \text{Per}(D_{ij}^{n,k}) + \delta_{lj} \text{Per}(D_{im}^{n,k}) + \delta_{im} \text{Per}(D_{lj}^{n,k}) - \delta_{lj} \delta_{im} \text{Per}(\Omega^{n,k}) \\ + k \xi_{2l} \left\{ n \xi_{1m}^* \left[\delta_{ij} \text{Per}(\mathcal{O}_{1d}^{n,k}) + n \xi_{1i} \left(k \xi_{2j}^* \text{Per}(\Omega^{n-1,k-1}) + (n-1) \xi_{1j}^* \text{Per}(\mathcal{O}_{1d}^{n-1,k}) \right) \right] \right. \\ \left. + (k-1) \xi_{2i} \left((n-1) \xi_{1j}^* \text{Per}(\mathcal{O}_{2d}^{n,k}) + k \xi_{2j}^* \text{Per}(\mathcal{O}_{1d}^{n,k-1}) \right) \right\} + k \xi_{2m}^* \text{Per}(D_{ij}^{n,k-1}) \\ + n \xi_{1l} \left\{ k \xi_{2m}^* \left[\delta_{ij} \text{Per}(\mathcal{O}_{1u}^{n,k}) + k \xi_{2i} \left(n \xi_{1j}^* \text{Per}(\Omega^{n-1,k-1}) + (k-1) \xi_{2j}^* \text{Per}(\mathcal{O}_{1u}^{n,k-1}) \right) \right] \right. \\ \left. + (n-1) \xi_{1i} \left((k-1) \xi_{2j}^* \text{Per}(\mathcal{O}_{2u}^{n,k}) + n \xi_{1j}^* \text{Per}(\mathcal{O}_{1u}^{n-1,k}) \right) \right\} + n \xi_{1m}^* \text{Per}(D_{ij}^{n-1,k}). \end{aligned} \quad (32)$$

Now we are in the position to calculate analytically, in terms of the Jacobi polynomials, several quantities, like the total energy, the number fluctuations, the decay rate when the system is coupled to an external environment and the coherence visibility.

A. Energy

Supposing that our system is described by the Hamiltonian given in Eq. (14), we can calculate the energy of our many body state, Eq. (9), as follows

$$\begin{aligned} E = \langle H \rangle = -\frac{t}{2} \left(\frac{\text{Per}(D_{LR}^{n,k}) + \text{Per}(D_{RL}^{n,k})}{\text{Per}(\Omega^{n,k})} \right) + \frac{U}{2} \left(\frac{\text{Per}(I_{LLLL}^{n,k}) + \text{Per}(I_{RRRR}^{n,k})}{\text{Per}(\Omega^{n,k})} \right) \\ + (\mu - 2U) \frac{\text{Per}(D_{LL}^{n,k})}{\text{Per}(\Omega^{n,k})} - (\mu + 2U) \frac{\text{Per}(D_{RR}^{n,k})}{\text{Per}(\Omega^{n,k})} + 2U. \end{aligned} \quad (33)$$

B. Number fluctuations

In the same manner we can calculate the charge fluctuations, for example on the left site,

$$\sigma_L = \langle n_L^2 \rangle - \langle n_L \rangle^2, \quad (34)$$

as the variance of the number operator, where

$$\langle n_L^2 \rangle = \frac{\langle \psi | a_L^\dagger a_L a_L^\dagger a_L | \psi \rangle}{\langle \psi | \psi \rangle} = \frac{\text{Per}(I_{LLLL}^{n,k}) - 3\text{Per}(D_{LL}^{n,k})}{\text{Per}(\Omega^{n,k})} + 1, \quad (35)$$

$$\langle n_L \rangle^2 = \left(\frac{\langle \psi | a_L^\dagger a_L | \psi \rangle}{\langle \psi | \psi \rangle} \right)^2 = \left(\frac{\text{Per}(D_{LL}^{n,k})}{\text{Per}(\Omega^{n,k})} - 1 \right)^2. \quad (36)$$

Analogously one can write the charge fluctuations on the right site, namely σ_R .

C. Decay rate

In this subsection we suppose our system weakly coupled to an external environment, therefore the total Hamiltonian is [32]

$$H_T = H + H_B + \lambda \left(W \hat{B} + W^\dagger \hat{B}^\dagger \right), \quad (37)$$

where H_B is the environment Hamiltonian while the last term is the weak coupling between the bath and the bosons, i.e. $\lambda \ll 1$. W is a bosonic operator. The heat bath acts as a source of noise and dissipation. We assume the environment to be in an equilibrium state and that behaves like a white noise, $\langle \hat{B}(t)^\dagger \hat{B} \rangle_E \simeq \delta(t)$. The presence of the bath leads to a master equation for the density matrix, $\rho = \frac{|\psi\rangle\langle\psi|}{\langle\psi|\psi\rangle}$, of the Kossakowski-Lindblad form [33]

$$\partial_t \rho = -i[H + H^{(2)}, \rho] + \mathcal{D}[\rho], \quad (38)$$

where

$$\begin{aligned} \mathcal{D}[\rho] = & \gamma \left(W \rho W^\dagger - \frac{1}{2} \{W^\dagger W, \rho\} \right) + \delta \left(W^\dagger \rho W - \frac{1}{2} \{W W^\dagger, \rho\} \right) \\ & + \beta \left(W \rho W - \frac{1}{2} \{W^2, \rho\} \right) + \beta^* \left(W^\dagger \rho W^\dagger - \frac{1}{2} \{W^{\dagger 2}, \rho\} \right), \end{aligned} \quad (39)$$

with $\gamma = \lambda^2 \int_{-\infty}^{+\infty} dx \langle \hat{B}^\dagger(x) \hat{B} \rangle_E$, $\delta = \lambda^2 \int_{-\infty}^{+\infty} dx \langle \hat{B}(x) \hat{B}^\dagger \rangle_E$, and $\beta = \lambda^2 \int_{-\infty}^{+\infty} dx \langle \hat{B}(x) \hat{B} \rangle_E$, some coefficients, $\beta \in \mathbb{C}$, $\gamma \geq 0$, $\delta \geq 0$, satisfying the condition $\gamma \delta \geq |\beta|^2$, which ensures the complete positivity (see Ref. [32] for more details). These coefficients incorporate the dissipative effects on the dynamics. The term $H^{(2)}$, is an environment induced additional Hamiltonian term whose explicit expression is not important for our purposes. Here, in fact,

we focus our attention to the stability of our initial pure state $\frac{|\psi\rangle\langle\psi|}{\langle\psi|\psi\rangle}$ at $t = 0$, calculating the constant decay rate defined by

$$\Gamma = -\left.\frac{\langle\psi|\partial_t\rho|\psi\rangle}{\langle\psi|\psi\rangle}\right|_{t=0} = -\frac{\langle\psi|\mathcal{D}[|\psi\rangle\langle\psi|]|\psi\rangle}{\langle\psi|\psi\rangle^2} = \gamma\Gamma_\gamma + \delta\Gamma_\delta + 2\text{Re}[\beta\Gamma_\beta], \quad (40)$$

where

$$\Gamma_\gamma = \frac{\langle\psi|W^\dagger W|\psi\rangle}{\langle\psi|\psi\rangle} - \left|\frac{\langle\psi|W|\psi\rangle}{\langle\psi|\psi\rangle}\right|^2 \quad (41)$$

$$\Gamma_\delta = \frac{\langle\psi|WW^\dagger|\psi\rangle}{\langle\psi|\psi\rangle} - \left|\frac{\langle\psi|W|\psi\rangle}{\langle\psi|\psi\rangle}\right|^2 \quad (42)$$

$$\Gamma_\beta = \frac{\langle\psi|WW|\psi\rangle}{\langle\psi|\psi\rangle} - \left(\frac{\langle\psi|W|\psi\rangle}{\langle\psi|\psi\rangle}\right)^2 \quad (43)$$

Let us choose W as a generic single particle operator, linear combination of an hopping term and right and left density operators

$$W = c_L n_L + c_R n_R + c_h a_R^\dagger a_L. \quad (44)$$

Usually only the hopping operator is considered in the coupling with the bath [11], i.e. $c_R = c_L = 0$. Here, instead, we consider a more general operator. Without loss of generality and without spoiling the complete positivity, we could put $\beta = 0$ and consider only Γ_γ or Γ_δ to show how the decay rate scales with the number of bosons. We have therefore

$$\begin{aligned} \Gamma_\gamma &= |c_L|^2 \sigma_L + |c_R|^2 \sigma_R + |c_h|^2 \Gamma_\gamma^h + 2\text{Re}(c_L c_R^*) (\langle n_L n_R \rangle - \langle n_L \rangle \langle n_R \rangle) \\ &\quad + c_L c_h^* (\langle n_L a_L^\dagger a_R \rangle - \langle n_L \rangle \langle a_L^\dagger a_R \rangle) + c_h c_L^* (\langle a_R^\dagger a_L n_L \rangle - \langle n_L \rangle \langle a_R^\dagger a_L \rangle) \\ &\quad + c_R c_h^* (\langle n_R a_L^\dagger a_R \rangle - \langle n_R \rangle \langle a_L^\dagger a_R \rangle) + c_h c_R^* (\langle a_R^\dagger a_L n_R \rangle - \langle n_R \rangle \langle a_R^\dagger a_L \rangle) \end{aligned} \quad (45)$$

where $\langle \dots \rangle \equiv \frac{\langle \psi | \dots | \psi \rangle}{\langle \psi | \psi \rangle}$, σ_L and σ_R are defined by Eq. (34) and

$$\Gamma_\gamma^h = \langle a_L^\dagger a_R a_R^\dagger a_L \rangle - |\langle a_L a_R^\dagger \rangle|^2 = \frac{\text{Per}(I_{LRR}^{n,k}) - \text{Per}(D_{LL}^{n,k})}{\text{Per}(\Omega^{n,k})} - \left| \frac{\text{Per}(D_{LR}^{n,k})}{\text{Per}(\Omega^{n,k})} \right|^2 \quad (46)$$

which is the common γ -contribution to the decay rate when the bath induces only hopping of particle between the two sites [11]. When the environment couples also to the local densities we have to calculate, in addition,

$$\langle n_L n_R \rangle - \langle n_L \rangle \langle n_R \rangle = \frac{\text{Per}(I_{LRL}^{n,k})}{\text{Per}(\Omega^{n,k})} - \frac{\text{Per}(D_{LL}^{n,k})\text{Per}(D_{RR}^{n,k})}{\text{Per}(\Omega^{n,k})^2}, \quad (47)$$

$$\langle n_L a_L^\dagger a_R \rangle - \langle n_L \rangle \langle a_L^\dagger a_R \rangle = \frac{\text{Per}(I_{LRL}^{n,k})}{\text{Per}(\Omega^{n,k})} - \frac{\text{Per}(D_{LR}^{n,k})}{\text{Per}(\Omega^{n,k})} - \left(\frac{\text{Per}(D_{LL}^{n,k})}{\text{Per}(\Omega^{n,k})} - 1 \right) \frac{\text{Per}(D_{RL}^{n,k})}{\text{Per}(\Omega^{n,k})}, \quad (48)$$

$$\langle n_R a_L^\dagger a_R \rangle - \langle n_R \rangle \langle a_L^\dagger a_R \rangle = \frac{\text{Per}(I_{RRL}^{n,k})}{\text{Per}(\Omega^{n,k})} - 2 \frac{\text{Per}(D_{LR}^{n,k})}{\text{Per}(\Omega^{n,k})} - \left(\frac{\text{Per}(D_{RR}^{n,k})}{\text{Per}(\Omega^{n,k})} - 1 \right) \frac{\text{Per}(D_{RL}^{n,k})}{\text{Per}(\Omega^{n,k})}, \quad (49)$$

and conjugate terms. Analogous calculations can be done for Γ_δ and Γ_β .

D. Visibility

In cold atom physics, in order to detect the coherence properties of the condensates, the quantity which are commonly used is the momentum distribution, namely the Fourier transform of the one-body density matrix $C(x, x') = \langle a(x)^\dagger a(x') \rangle$, where the brackets mean the ground state average. It has been shown [34–36] that the momentum distribution, $n(p) = \int dx dx' e^{-ip(x-x')} C(x, x')$, can be written as $n(p) = n_0(p)(1 + \alpha \cos(pd))$, where $n_0(p)$ is the momentum distribution in the incoherent regime which depends on the details of the feasible double-well potential, d the distance of the two minima of the double-well and α the so-called visibility. In terms of our site-operators, the visibility can be defined by

$$\alpha = \frac{2|\langle a_L^\dagger a_R \rangle|}{N}, \quad (50)$$

which, if valuated using our permanent states, is simply given by

$$\alpha = \frac{2}{N} \left| \frac{\text{Per}(D_{RL}^{n,k})}{\text{Per}(\Omega^{n,k})} \right|. \quad (51)$$

V. FOCK LIMIT, $\omega = 0$

Here and in what follows we put $b = 1$, namely we fix the normalization of the single particle wavefunctions. For $\omega = 0$ we have $\text{Per}(\mathcal{O}_{1u}) = \text{Per}(\mathcal{O}_{1d}) = \text{Per}(\mathcal{O}_{2u}) = \text{Per}(\mathcal{O}_{d2}) = 0$ while ${}_2F_1(-n, -k, 1; 0) = 1, \forall n, k$, therefore

$$\text{Per}(\Omega^{n,k}) = n!k!, \quad (52)$$

$$\text{Per}(D_{ij}^{n,k}) = n!k! (\delta_{ij} + n\xi_{1j}^* \xi_{1i} + k\xi_{2j}^* \xi_{2i}), \quad (53)$$

$$\begin{aligned} \text{Per}(I_{lijm}^{n,k}) = n!k! & \left[\delta_{ij} \delta_{lm} + \delta_{im} \delta_{lj} + n (\delta_{lm} \xi_{2j}^* \xi_{2i} + \delta_{im} \xi_{2j}^* \xi_{2l} + \delta_{lj} \xi_{2m}^* \xi_{2i} + \delta_{ij} \xi_{2m}^* \xi_{2l}) \right. \\ & + k (\delta_{lm} \xi_{1j}^* \xi_{1i} + \delta_{im} \xi_{1j}^* \xi_{1l} + \delta_{lj} \xi_{1m}^* \xi_{1i} + \delta_{ij} \xi_{1m}^* \xi_{1l}) + (n^2 - n) \xi_{1i} \xi_{1j}^* \xi_{1l} \xi_{1m}^* \\ & \left. + (k^2 - k) \xi_{2i} \xi_{2j}^* \xi_{2l} \xi_{2m}^* + nk (\xi_{1l} \xi_{2i} + \xi_{1i} \xi_{2l}) (\xi_{1m}^* \xi_{2j}^* + \xi_{1j}^* \xi_{2m}^*) \right]. \quad (54) \end{aligned}$$

The charge fluctuations, then, reads

$$\sigma_L = n|\xi_{1L}|^2 |\xi_{1R}|^2 + k|\xi_{2L}|^2 |\xi_{2R}|^2 + 2nk|\xi_{1L}|^2 |\xi_{2L}|^2, \quad (55)$$

and the decay rate Γ_γ^h , given by Eq. (46), is simply

$$\Gamma_\gamma^h = n|\xi_{1L}|^4 + k|\xi_{2L}|^4 + nk (|\xi_{1R}|^2 |\xi_{2L}|^2 + |\xi_{2R}|^2 |\xi_{1L}|^2), \quad (56)$$

where, of course $|\xi_{\alpha L}|^2 + |\xi_{\alpha R}|^2 = 1$ is understood. So far we have used only $\omega = 0$, which is a necessary but not sufficient condition for having spatially separated Fock state, as we will see in Sec.VIII.A.4. Now, choosing the Fock state as follows

$$|\psi_F\rangle = \left(\xi_{1L} a_L^\dagger \right)^n \left(\xi_{2R} a_R^\dagger \right)^k |0\rangle, \quad (57)$$

we are forced to put $\xi_{1i} = \delta_{iL}$ and $\xi_{2i} = \delta_{iR}$ in Eqs. (53, 54). This implies that the occupation numbers are $\langle n_L \rangle = n$ and $\langle n_R \rangle = k$, and the energy, the charge fluctuations, the visibility and the decay rate are simply given by

$$E = \frac{U}{2}(n(n-1) + k(k-1)) + \mu(n-k), \quad (58)$$

$$\sigma_L = \sigma_R = 0, \quad (59)$$

$$\alpha = 0, \quad (60)$$

$$\Gamma_\gamma = |c_h|^2 n(k+1), \quad (61)$$

and, analogously, $\Gamma_\delta = |c_h|^2 k(n+1)$ and $\Gamma_\beta = |c_h|^2 (n+1)(k+1)$. The decay rate, in the Fock limit, is, therefore, $\propto N^2/4$, for $n \simeq k \simeq N/2$, and is due only to the coupling of the bath with the hopping-like term.

VI. COHERENT LIMIT, $\omega = 1$

For $\omega = 1$ we have that

$${}_2F_1(-n, -k, 1; 1) = \binom{n+k}{n}, \quad (62)$$

$$\sum_{\ell=0}^{k-1} {}_2F_1(1-n, -\ell, 1; 1) = \binom{n+k-1}{n}, \quad (63)$$

$$\sum_{m=0}^{n-2} (1+m) \sum_{\ell=0}^{k-2} {}_2F_1(-m, -\ell, 1; 1) = \frac{n(n-1)}{k} \binom{n+k-2}{n}. \quad (64)$$

We get, therefore, the following simple expressions

$$\text{Per}(\Omega^{n,k}) = (n+k)!, \quad (65)$$

$$\text{Per}(\mathcal{O}_{1u}^{n,k}) = \text{Per}(\mathcal{O}_{1d}^{n,k}) = (n+k-1)!, \quad (66)$$

$$\text{Per}(\mathcal{O}_{2u}^{n,k}) = \text{Per}(\mathcal{O}_{2d}^{n,k}) = (n+k-2)!. \quad (67)$$

The coherent state is obtained when

$$\xi_L \equiv \xi_{1L} = \xi_{2L}, \quad (68)$$

$$\xi_R \equiv \xi_{1R} = \xi_{2R}, \quad (69)$$

so that Eq. (9) reduces to

$$|\psi_C\rangle = \left(\xi_L a_L^\dagger + \xi_R a_R^\dagger \right)^N |0\rangle, \quad (70)$$

where $N = (n+k)$, the total number of bosons, and $|\xi_L|^2 + |\xi_R|^2 = 1$. In the coherent case we obtain, therefore, simply

$$\text{Per}(D_{ij}^{n,k}) = N! \{ \delta_{ij} + N \xi_i \xi_j^* \}, \quad (71)$$

$$\begin{aligned} \text{Per}(I_{lijm}^{n,k}) = N! \{ & \delta_{ij} \delta_{ml} + \delta_{jl} \delta_{im} + N (\delta_{lj} \xi_i \xi_m^* + \delta_{lm} \xi_i \xi_j^* + \delta_{ij} \xi_l \xi_m^* + \delta_{im} \xi_l \xi_j^*) \\ & + (N^2 - N) \xi_l \xi_i \xi_j^* \xi_m^* \}. \end{aligned} \quad (72)$$

Notice that Eqs. (71) and (72) are valid also for a lattice, namely, in the presence of many sites, when the state is given by $|\psi\rangle = \left(\sum_i^{N_s} \xi_i a_i^\dagger\right)^N |0\rangle$. From Eq. (71) we get that the occupation numbers are the following

$$\langle n_L \rangle = N|\xi_L|^2, \quad (73)$$

$$\langle n_R \rangle = N|\xi_R|^2. \quad (74)$$

Energy, charge fluctuations, visibility and decay rate are given by

$$E = -\frac{t}{2} (\xi_L \xi_R^* + \xi_R \xi_L^*) N + \mu N (|\xi_L|^2 - |\xi_R|^2) + \frac{U}{2} (|\xi_L|^4 + |\xi_R|^4) N(N-1), \quad (75)$$

$$\sigma = \sigma_L = \sigma_R = N|\xi_L|^2 |\xi_R|^2, \quad (76)$$

$$\alpha = 2|\xi_R \xi_L^*|, \quad (77)$$

$$\Gamma_\gamma = N \{ |c_L - c_R|^2 |\xi_L|^2 |\xi_R|^2 + |c_h|^2 |\xi_R|^4 + 2\text{Re}[(c_L |\xi_L|^2 - c_R |\xi_R|^2) c_h^* \xi_R \xi_L^*] \}, \quad (78)$$

and analogously, $\Gamma_\delta = N \{ |c_L - c_R|^2 |\xi_L|^2 |\xi_R|^2 + |c_h|^2 |\xi_L|^4 - 2\text{Re}[(c_L |\xi_L|^2 - c_R |\xi_R|^2) c_h^* \xi_R \xi_L^*] \}$. What we found is, therefore, that, in the coherent regime, both the number fluctuations and the decay rate scale linearly with the number of bosons, no matter how the bath is coupled with the bosons. The couplings affect only the prefactor of the decay rate. Before we conclude this section we present here a couple of interesting effects which are supposed to occur in the coherent-like regime.

A. Self-trapping

Let us consider small interaction so that the coherent state still well approximates the ground state or suppose that we can prepare the system in such a state. After defining the variables z , the relative charge imbalance, and ϕ , the phase difference between the left and right amplitudes,

$$z \equiv (\langle n_L \rangle - \langle n_R \rangle) / N = |\xi_L|^2 - |\xi_R|^2, \quad (79)$$

$$e^{i\phi} \equiv \frac{\xi_L \xi_R^*}{|\xi_L| |\xi_R|}, \quad (80)$$

we can rewrite the total energy Eq. (75), as follows

$$E = -\frac{t}{2} N \sqrt{1-z^2} \cos \phi + \frac{U}{4} N(N-1)(1+z^2) + \mu N z. \quad (81)$$

Eq. (81) is the Josephson energy, where the hopping term is proportional to $\cos \phi$. The effective Hamiltonian describing the evolution of z is $\mathcal{H} = E/N$ which gives the following equations of motion [23, 24, 37]

$$\dot{z} = \frac{t}{2} \sqrt{1-z^2} \sin \phi, \quad (82)$$

$$\dot{\phi} = \frac{Uz}{2} (N-1) - \frac{tz \cos \phi}{2\sqrt{1-z^2}} - \mu. \quad (83)$$

The Josephson current is, therefore, $I_J = N\dot{z} = \frac{tN^2}{2}\sqrt{1-z^2}\sin\phi$. For $\mu \rightarrow 0$, we get the following non-trivial fixed points

$$z = \pm \frac{\sqrt{U^2(N-1)^2 - t^2}}{U(N-1)}, \quad (84)$$

$$\phi = 0, \pm\pi, \quad (85)$$

which means that, for a particular imbalance, the particles do not arrange themselves to reach the symmetric configuration.

B. Attractive interaction: Symmetry breaking

We now consider the attractive interacting case, $U < 0$, supposing that the state remains coherent also for negative U , not only strictly for zero interaction. The total energy of a coherent state is given by Eq. (75). The energy profile, for $\mu = 0$ and $\phi = 0$, has only one minimum at

$$|\xi_L|^2 = \frac{1}{2}, \quad \text{for } \frac{t}{1-N} \leq U \leq 0, \quad (86)$$

while develops two minima at

$$|\xi_L|^2 = \frac{1}{2} \pm \frac{\sqrt{U^2(N-1)^2 - t^2}}{2U(N-1)}, \quad \text{for } U < \frac{t}{1-N}. \quad (87)$$

For $U < \frac{t}{1-N}$, then, the ground state becomes twice degenerate and the charge imbalance, $z = 2|\xi_L|^2 - 1$, is finite, given again by Eq. (84).

VII. LARGE N LIMIT, $\omega \in (0, 1]$

In this section we derive the asymptotic behavior of the charge fluctuations and of the decay rate in the large N limit. The result is valid as long as

$$|\omega| \gg N^{-1} \quad (88)$$

and for $k = n = N/2$. In this case we obtain the following asymptotic behaviors for the permanents appearing in the correlators, Eqs. (30, 32),

$$\text{Per}(\Omega^{n-1,n}) = \text{Per}(\Omega^{n,n}) \left[\frac{1 - |\omega| + 4n}{4(1 + |\omega|)n^2} + O(n^{-3}) \right], \quad (89)$$

$$\text{Per}(\mathcal{O}_{1u}^{n,n}) = \text{Per}(\Omega^{n,n}) \left[\frac{|\omega| - 1 + 4|\omega|n}{4\omega^*(1 + |\omega|)n^2} + O(n^{-3}) \right], \quad (90)$$

$$\text{Per}(\mathcal{O}_{2u}^{n,n}) = \text{Per}(\Omega^{n,n}) \left[\frac{2\omega^2(|\omega| - 1 + |\omega|n)}{|\omega|^3(1 + |\omega|)^2(2n-1)n^2} + O(n^{-4}) \right], \quad (91)$$

$$\text{Per}(\Omega^{n-2,n}) = \text{Per}(\Omega^{n,n}) \left[\frac{2 - 2|\omega| + 2n}{(1 + |\omega|)^2(2n-1)n^2} + O(n^{-4}) \right], \quad (92)$$

$$\text{Per}(\Omega^{n-1,n-1}) = \text{Per}(\Omega^{n,n}) \left[\frac{2}{(1 + |\omega|)^2(2n-1)n} + O(n^{-4}) \right], \quad (93)$$

and $\text{Per}(\mathcal{O}_{1d}^{n,n}) = \text{Per}(\mathcal{O}_{1u}^{n,n})^*$, $\text{Per}(\Omega^{n,n-1}) = \text{Per}(\overline{\Omega}^{n-1,n})$, $\text{Per}(\Omega^{n,n-2}) = \text{Per}(\Omega^{n-2,n})$. Notice that for $\omega = 1$ only the leading terms survive and we recover the exact results for the coherent states, Eqs. (65-67).

Using these relations we can calculate the charge fluctuation and the decay rate. For simplicity we now choose all ξ 's real so that ω is also real. Since we are considering the simple case with $k = n$, namely a symmetrically occupied double well, we can use the following parametrization

$$\xi_{1L} = \xi_{2R} = \frac{1}{\sqrt{2}} \sqrt{1 + \sqrt{1 - \omega^2}}, \quad (94)$$

$$\xi_{2L} = \xi_{1R} = \frac{1}{\sqrt{2}} \sqrt{1 - \sqrt{1 - \omega^2}}, \quad (95)$$

which fulfils the normalization conditions and the definition of the single particle overlap. We have also checked that, for $\mu = 0$ and repulsive interaction, $U \geq 0$, the balance conditions ($k = n$ and $\xi_{1L} = \xi_{2R}$, $\xi_{1R} = \xi_{2L}$) naturally minimize the total energy. After this parametrization we can calculate, for instance, σ and Γ_γ , and, after expanding in N^{-1} , we obtain, at the leading order,

$$\sigma_L = \sigma_R = \sigma \simeq \frac{\omega N}{4}, \quad (96)$$

$$\Gamma_\gamma \simeq \frac{N}{4} \left| \frac{c_h}{\sqrt{\omega}} + \sqrt{\omega}(c_L - c_R) \right|^2, \quad (97)$$

and, analogously, $\Gamma_\delta \simeq \frac{N}{4} \left| \frac{c_h}{\sqrt{\omega}} - \sqrt{\omega}(c_L - c_R) \right|^2$. Calculating the total energy, Eq. (33), with the asymptotics written above, Eqs. (89)-(93), we obtain

$$E = \frac{U \left(8 + 4\omega(\omega^2 - 3) - 2N + 2\omega(4 + \omega - 2\omega^2)N + N^2(1 + \omega)^2(N + \omega - 3) \right)}{4(1 + \omega)^2(N - 1)} + \frac{t}{4\omega} \left(1 + \omega^2 - 2\omega(N + 1) \right), \quad (98)$$

and imposing $\delta_\omega E = 0$, we get the minimum energy when

$$\omega_o \simeq \frac{\sqrt{t}}{\sqrt{t + NU}}, \quad (99)$$

which is consistent with the limit $\omega \sim N^{-1/2} \gg N^{-1}$ the asymptotic is based on. As a result, the decay rate at $U = 0$, is

$$\Gamma_\gamma \simeq \frac{N}{4} |c_L - c_R + c_h|^2 \quad (100)$$

and $\Gamma_\delta \simeq \frac{N}{4} |c_L - c_R - c_h|^2$. For U/t of order one and for large N , instead, the leading term is given by

$$\Gamma_\gamma \simeq \frac{N |c_h|^2}{4\omega_o} \simeq \frac{|c_h|^2}{4} \sqrt{\frac{U}{t}} N^{3/2}. \quad (101)$$

We know that $\Gamma_\gamma \simeq N^2|c_h|^2/4$ for the Fock states, meaning that when $\omega_o \sim N^{-1}$, which implies $U \sim tN$, namely, when the interaction is of order N , we enter the Fock regime. The charge fluctuations, far from the Fock regime, are

$$\sigma \simeq \frac{\omega_o N}{4} \simeq \frac{1}{4} \sqrt{\frac{t}{U}} N^{1/2}. \quad (102)$$

For $U = 0$, namely $\omega_o = 1$, we recover the result of Sec. VI, with $|\xi_L| = |\xi_R| = 1/\sqrt{2}$, since, without interaction, the coherent state is the ground state. Finally, making an expansion in N^{-1} of the total energy, Eq. (98), calculated at the minimum, Eq. (99), we get

$$E_o = -\frac{t}{2}N + \frac{1}{4}UN(N-2) + \frac{1}{2}\sqrt{tUN} + O(1), \quad (103)$$

which, in spite of its simplicity, is a very good approximation of the ground state energy for intermediate interaction, i.e. $\frac{1}{N} \ll \frac{U}{t} \ll N$. By exactly diagonalizing the Hamiltonian for different values of N , in fact, one can easily check that Eq. (103) deviates from the exact ground level E_{ex} by an error, $E_o - E_{ex}$, of order $O(1) \approx (\frac{t}{2} + \frac{U}{16})$ (relative error of order $O(N^{-2})$). Notice that the coherent energy, $E_C = -\frac{t}{2}N + \frac{U}{4}N(N-1)$, deviates from the exact one by an error $O(N) \approx \frac{U}{4}N$ and the Fock energy, $E_F = \frac{U}{4}N(N-2)$, by an error $O(N) \approx \frac{t}{2}N$ (both relative errors of order $O(N^{-1})$). As a result, Eq. (103) can be considered as a non-perturbative analytical expression of the ground state energy for intermediate interaction.

Let us finally, consider the visibility, Eq. (51). This quantity is equal to 1 in the coherent-like state ($U = 0$) and decreases by increasing the repulsive interaction ($U > 0$). Using Eq. (30) and Eqs. (89), (90), for $n = k = N/2$, and Eqs. (94), (95), we obtain, in fact, for $0 \leq U/t \ll N$, at the leading orders,

$$\alpha \simeq 1 - \frac{(\omega_o - 1)^2}{2\omega_o N} \simeq 1 - \frac{(\sqrt{t} - \sqrt{t + NU})^2}{2N\sqrt{t(t + NU)}}. \quad (104)$$

This result for the coherence visibility is in a very good agreement with numerical results [28]. To conclude, both the energy, Eq. (103), and the visibility, Eq. (104), have been successfully compared with exact diagonalization results, validating therefore our ansatz of the interpolating state in the regime of repulsive interaction.

VIII. ENTANGLEMENT FOR $U \geq 0$

In this section, we conclude our study calculating the entanglement entropy and the Fisher information of our permanent state.

A. Entropy

Given the wavefunction (9), we can derive the reduced density matrix for the left site, for instance, by tracing out the right one (for a review, see Ref. [29] and references therein)

$$\hat{\rho} = \frac{1}{\langle \psi | \psi \rangle} \text{Tr}_R (|\psi\rangle\langle\psi|), \quad (105)$$

where Tr_R is the trace over the right site. More explicitly, we have to perform the following summation

$$\hat{\rho} = \frac{1}{\langle \psi | \psi \rangle} \sum_{m=0}^{n+k} \frac{1}{m!} \langle 0 | (a_R)^m | \psi \rangle \langle \psi | (a_R^\dagger)^m | 0 \rangle. \quad (106)$$

This is a diagonal $(n+k+1) \times (n+k+1)$ matrix, $\rho_{\ell\ell'} = \rho_\ell \delta_{\ell\ell'}$, whose diagonal elements can be written analytically as follows

$$\rho_\ell = \frac{|\xi_{2L}|^{2n} |\xi_{1R}|^{2\ell} |\xi_{2R}|^{2(k-\ell)} (n+k-\ell)! k! \left| {}_2F_1 \left(-n, -\ell, 1-\ell+k; \frac{\xi_{1L}\xi_{2R}}{\xi_{1R}\xi_{2L}} \right) \right|^2}{n! \ell! ((k-\ell)!)^2 {}_2F_1 \left(-n, -k, 1; |\xi_{2L}\xi_{1L}^* + \xi_{2R}\xi_{1R}^*| \right)}, \quad (107)$$

for $0 \leq \ell < k$ and

$$\rho_\ell = \frac{|\xi_{1L}|^{2(\ell-k)} |\xi_{2L}|^{2(n+k-\ell)} |\xi_{1R}|^{2k} \ell! n! \left| {}_2F_1 \left(\ell-n-k, -k, 1+\ell-k; \frac{\xi_{1L}\xi_{2R}}{\xi_{1R}\xi_{2L}} \right) \right|^2}{k! (n+k-\ell)! ((\ell-k)!)^2 {}_2F_1 \left(-n, -k, 1; |\xi_{2L}\xi_{1L}^* + \xi_{2R}\xi_{1R}^*| \right)}, \quad (108)$$

for $k \leq \ell \leq n+k$. The ξ 's are related by normalization conditions, Eq. (12). We can therefore calculate the von Neumann entropy

$$S = - \sum_{\ell=0}^{n+k} \rho_\ell \log_2 \rho_\ell \quad (109)$$

with \log_2 the logarithm to base 2. We have shown that also the reduced density matrix and the entropy can be written in terms of Jacobi polynomials of ω and of the ratio $\frac{\xi_{1L}\xi_{2R}}{\xi_{1R}\xi_{2L}}$.

1. Fock limit

In the Fock limit, $\omega = 0$, choosing $\xi_{1i} = \delta_{iR}$ and $\xi_{2i} = \delta_{iL}$ (the other choice is equivalent but one should take care of the ratio $\frac{\xi_{1L}\xi_{2R}}{\xi_{1R}\xi_{2L}}$, the argument of the Jacobi polynomial appearing in the numerator of the density matrix), from Eqs. (107), (108), we get

$$\rho_\ell = \delta_{\ell k}. \quad (110)$$

As a consequence the entropy is simply $S = 0$.

2. Coherent limit

If $\xi_{1L} = \xi_{2L}$ and $\xi_{1R} = \xi_{2R}$, then $\omega = 1$, and the reduced density matrix becomes simply

$$\rho_\ell = \binom{N}{\ell} |\xi_L|^{2\ell} |\xi_R|^{2(N-\ell)}, \quad (111)$$

where, of course, $N = n + k$ and $|\xi_R|^2 = (1 - |\xi_L|^2)$. In this case we can calculate the asymptotic behavior of the von Neumann entropy for $N \gg 1$, since the binomial distribution, Eq. (111), approaches the gaussian one

$$\rho_\ell \simeq \frac{1}{\sqrt{2\pi N |\xi_L|^2 |\xi_R|^2}} \exp \left[-\frac{(\ell - N |\xi_L|^2)^2}{2N |\xi_L|^2 |\xi_R|^2} \right], \quad (112)$$

obtaining the following asymptotic behavior for the entropy [31]

$$S \simeq \frac{1}{2} \log_2 (2\pi e N |\xi_L|^2 |\xi_R|^2). \quad (113)$$

3. Intermediate case, with $n = k$

Now let us consider the case of $k = n = N/2$ and Eqs. (94), (95). Applying Eqs. (107), (108) and (109) we get an entropy which is well approximated, for $\omega \gg 1/N$, by

$$S \approx \frac{1}{2} \log_2 \left(\pi e \omega \frac{N}{2} \right), \quad (114)$$

as one can see from Fig. (1). At $\omega = \omega_o$, for U/t of order one, we get $S \sim \frac{1}{4} \log_2(N) + \text{const.}$

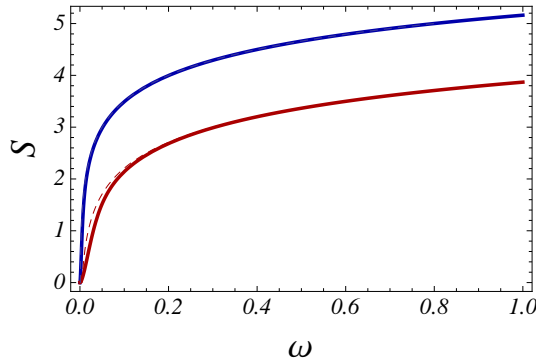


FIG. 1: (Color online) Entanglement entropy, S , in the repulsive regime, as a function of ω , for $N = 300$ (upper solid line) and $N = 50$ (lower solid line). The dashed lines are the approximated behaviors given by Eq. (114), for $N = 300$ (upper dashed line, which cannot be distinguished from the solid line) and $N = 50$ (lower dashed line), which deviates from the solid line only for small ω .

4. *A special case: an almost maximally entangled state*

In this paragraph we will consider a simple state which has the same functional form of Eq. (9), with same amplitudes in modulus, obtained by a phase deformation of the balanced coherent-like state. We will show that the phase can be tuned in order to get an almost maximally entangled state. Let us consider, therefore, Eq. (9), with

$$\xi_{1L} = \xi_{2L} = \xi_{1R} = e^{-i\phi}\xi_{2R} = 1/\sqrt{2}, \quad (115)$$

such that the not normalized state reads

$$|\psi\rangle = \frac{1}{\sqrt{2^{n+k}}} \left(a_L^\dagger + a_R^\dagger\right)^n \left(a_L^\dagger + e^{i\phi}a_R^\dagger\right)^k |0\rangle, \quad (116)$$

then the overlap parameter is given by

$$\omega = \frac{1}{2}(1 + e^{i\phi}). \quad (117)$$

When $\phi = 0$ we recover the coherent state. Using Eqs. (107), (108) and (109) one can verify that the state in Eq. (116) is more entangled than the fully delocalized coherent state, i.e. $S(\phi \neq 0) > S(\phi = 0)$, as we can see in Fig. 2.

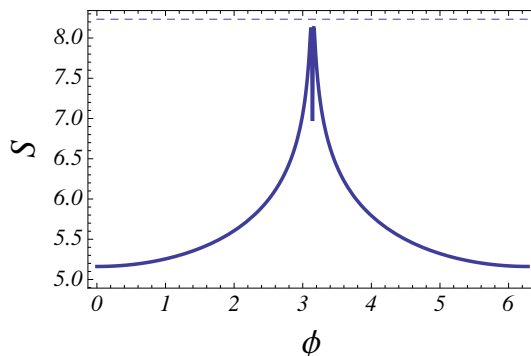


FIG. 2: (Color online) Entanglement entropy for the state in Eq. (116), with $n = k = N/2$, as a function of ϕ . For $N = 300$, the entropy reaches its maximum at $\phi = \pi \pm 0.02$ which is $S(\phi) \approx 8.13$. The dashed line is the upper limit entropy, $\log_2(N + 1)$, which, for $N = 300$, is ≈ 8.23 . Exactly at $\phi = \pi$ there is a narrow dip where $S(\phi = \pi) \approx 6.96$, nicely approximated by Eq. (122), which gives ≈ 7.23 . At $\phi = 0$ and 2π , the entropy coincides with Eq. (113), giving $S(\phi = 0) \approx 5.16$.

In particular, for $\phi = \pi$ the single particle overlap is $\omega = 0$, like the Fock state. Defining

$$a_1^\dagger = (a_L^\dagger + a_R^\dagger)/\sqrt{2}, \quad (118)$$

$$a_2^\dagger = (a_L^\dagger - a_R^\dagger)/\sqrt{2}, \quad (119)$$

the state in Eq. (116) is, indeed, a Fock state in the new representation, $|\psi\rangle = (a_1^\dagger)^n (a_2^\dagger)^k |0\rangle$, very unstable under coupling to an external bath, in fact $\Gamma_\gamma^h \simeq nk/2$ (see Eq. (56)), and, at

the same time, with a quite large number fluctuations, $\sigma \simeq nk/2$, (see Eq. (55)). For $\phi = \pi$ and $k = n = N/2$, the reduced density matrix is simply given by

$$\rho_{2\ell} = \frac{(2\ell)!(2n - 2\ell)!}{4^n (\ell!)^2 ((n - \ell)!)^2}, \quad (120)$$

$$\rho_{2\ell+1} = 0. \quad (121)$$

Studying the profile of the reduced density matrix, Eq. (120), one can check that, it can be approximated as $\rho_{2\ell} \approx 1/n = 2/N$, yielding, therefore, the following approximated value for the entropy

$$S \approx \log_2(N) - 1. \quad (122)$$

The state Eq. (116) with $\phi = \pi$ and $n = k$, is, therefore, almost double entangled with respect to the coherent state ($\phi = 0$), as one can see by comparing Eq. (122) with Eq. (113). In conclusion, the state in Eq. (116), at $\phi \approx \pi$, is almost maximally entangled since the entropy approaches the upper limit for N bosons, i.e. $\log_2(N + 1)$, as shown in Fig. 2. What shown is a simple example of how the entanglement can increase by losing coherence.

B. Fisher information

The Fisher information is defined by [28, 38–40]

$$F = \frac{\langle (n_L - n_R)^2 \rangle - \langle (n_L - n_R) \rangle^2}{N^2}, \quad (123)$$

which can be written as follows

$$F = \frac{1}{N^2} \{ \sigma_L + \sigma_R - 2(\langle n_L n_R \rangle - \langle n_L \rangle \langle n_R \rangle) \}. \quad (124)$$

If we consider the case with $n = k = N/2$, after choosing ξ real and parametrizing them as in Eqs. (94), (95) we get

$$F \simeq \frac{\omega^2}{2}, \quad (125)$$

for $\omega \ll N^{-1}$, and

$$F \simeq \frac{\omega}{N}, \quad (126)$$

for $\omega \gg N^{-1}$. The overlap of the bosons can be seen, therefore, as the parameter which encodes the quantum information. In the latter case, i.e. $\omega \gg N^{-1}$, we find, in fact, that, at least at the leading term,

$$\langle n_L n_R \rangle - \langle n_L \rangle \langle n_R \rangle \simeq -\sigma \quad (127)$$

where $\sigma = \sigma_L = \sigma_R$. Equation (127) becomes exact in the coherent limit, $\omega = 1$. This implies a very interesting relation, valid at least for $\omega \gg N^{-1}$,

$$F \simeq \frac{4\sigma}{N^2}. \quad (128)$$

For finite interaction and at the ground state energy, we know that $\omega_o \simeq \sqrt{t/(NU)}$, therefore, we get

$$F \simeq \sqrt{\frac{t}{U}} N^{-3/2}. \quad (129)$$

We notice that the Fisher information and the decay time $\tau_\gamma \equiv 1/\Gamma_\gamma$, for finite U/t , behave in the same way, namely they are proportional, i.e. $F \simeq \tau_\gamma |c_h|^2/4$, at least for a symmetrically occupied double well and large N . We can say, therefore, that the greater is the Fisher information, the longer the state survives under coupling to an external environment.

IX. ATTRACTIVE INTERACTION: THE SCHRÖDINGER CAT

In this section we will study the evolution from a coherent-like state to a *NOON* state, namely $|N\rangle_L|0\rangle_R + |0\rangle_L|N\rangle_R$, reached in the limit $U \rightarrow -\infty$. As we have seen before, this regime seems to be characterized by a symmetry breaking, as soon as $U < U_c$, where

$$U_c = -\frac{t}{(N-1)}. \quad (130)$$

We will consider, therefore, the following “cat” state, superposition of two unbalanced coherent-like states,

$$|\psi_{\text{cat}}\rangle = |\psi_L\rangle + |\psi_R\rangle, \quad (131)$$

with

$$|\psi_L\rangle = \left(\xi^> a_L^\dagger + \xi^< a_R^\dagger\right)^N |0\rangle, \quad (132)$$

$$|\psi_R\rangle = \left(\xi^< a_L^\dagger + \xi^> a_R^\dagger\right)^N |0\rangle. \quad (133)$$

where $|\xi^>| \geq |\xi^<|$, and $|\xi^>|^2 + |\xi^<|^2 = 1$, meaning that $|\psi_L\rangle$ is more weighted on the left site while $|\psi_R\rangle$ on the right site. After defining the charge imbalances for $|\psi_L\rangle$ and $|\psi_R\rangle$, one opposite to the other,

$$z = z_L = -z_R = |\xi^>|^2 - |\xi^<|^2, \quad (134)$$

the energy in the quantum coherent regime, can be written as in Eq. (81) (with $\mu = 0$). Imposing $\partial E/\partial z = 0$ and $\partial E/\partial \phi = 0$, we get two minima, for any $\phi = 2n\pi$,

$$z_o = \pm \frac{\sqrt{U^2(N-1)^2 - t^2}}{U(N-1)}, \quad (135)$$

as soon as $U < U_c$. The two solutions correspond to the state $|\psi_L\rangle$ or to the state $|\psi_R\rangle$. Actually, the energy is even reduced, as we will show in what follows, by taking the symmetric linear combination of those two states, which leads to the cat state written in Eq. (131). It describes a superposition of a cat sitting on the left site but with his tail on the right one and viceversa. When the cat withdraws the tail we get the *NOON* state.

In order to calculate the quantities of interest on the cat state, we first write the following correlators, with $|\psi_s\rangle = \{|\psi_L\rangle, |\psi_R\rangle\}$,

$$\langle \psi_s | \psi_{s'} \rangle = N! b_{s,s'}^N \equiv \text{Per}(\Omega^{N,0}(s, s')), \quad (136)$$

$$\langle \psi_s | a_i a_j^\dagger | \psi_{s'} \rangle = N! \left(\delta_{ij} b_{s,s'}^N + N b_{s,s'}^{N-1} \xi_i^s \xi_j^{s'*} \right) \equiv \text{Per}(D_{ij}^{N,0}(s, s')), \quad (137)$$

$$\begin{aligned} \langle \psi_s | a_l a_i a_j^\dagger a_m^\dagger | \psi_{s'} \rangle &= \delta_{lm} \text{Per}(D_{ij}^{N,0}(s, s')) + \delta_{lj} \text{Per}(D_{im}^{N,0}(s, s')) + \delta_{im} \text{Per}(D_{lj}^{N,0}(s, s')) \\ &\quad - \delta_{lj} \delta_{im} \text{Per}(\Omega^{N,0}(s, s')) + N^2 \xi_l^s \xi_m^{s'*} \text{Per}(D_{ij}^{N-1,0}(s, s')), \end{aligned} \quad (138)$$

where $s = L, R$ and

$$\xi_L^L = \xi_R^R = \xi^>, \quad (139)$$

$$\xi_L^L = \xi_L^R = \xi^<, \quad (140)$$

$$b_{L,L} = b_{R,R} = 1, \quad (141)$$

$$b_{L,R} = b_{R,L} = \xi^> \xi^{<*} + \xi^< \xi^{>*}. \quad (142)$$

The normalization of the cat state is, therefore, given by

$$\begin{aligned} \langle \psi_\oplus | \psi_\oplus \rangle &= 2N! \left[1 + (\xi^> \xi^{<*} + \xi^< \xi^{>*})^N \right] = 2N! \left[1 + \left(\sqrt{1-z^2} \cos \phi \right)^N \right] \Big|_{\phi=2n\pi} \\ &= 2N! \left[1 + \left(\sqrt{1-z^2} \right)^N \right]. \end{aligned} \quad (143)$$

Without loss of generality, choosing $\xi^>, \xi^<$ real, from Eqs. (137), (138), we get the following quantities, useful to calculate energy, Fisher information, number fluctuations and decay rates, all in terms of z , the imbalance parameter,

$$\langle a_L^\dagger a_R \rangle_\oplus = \langle a_R^\dagger a_L \rangle_\oplus \equiv \frac{\langle \psi_\oplus | a_R^\dagger a_L | \psi_\oplus \rangle}{\langle \psi_\oplus | \psi_\oplus \rangle} = \frac{N}{2} \left(\frac{\sqrt{1-z^2} + (\sqrt{1-z^2})^{N-1}}{1 + (\sqrt{1-z^2})^N} \right), \quad (144)$$

$$\langle n_L \rangle_\oplus = \langle n_R \rangle_\oplus \equiv \frac{\langle \psi_\oplus | a_L^\dagger a_L | \psi_\oplus \rangle}{\langle \psi_\oplus | \psi_\oplus \rangle} = \frac{N}{2}, \quad (145)$$

$$\langle n_L^2 \rangle_\oplus = \langle n_R^2 \rangle_\oplus \equiv \frac{\langle \psi_\oplus | a_L^\dagger a_L a_L^\dagger a_L | \psi_\oplus \rangle}{\langle \psi_\oplus | \psi_\oplus \rangle} = \frac{N}{2} + \frac{N}{4} (N-1) \left(1 + \frac{z^2}{1 + (\sqrt{1-z^2})^N} \right), \quad (146)$$

$$\langle n_L n_R \rangle_\oplus \equiv \frac{\langle \psi_\oplus | a_L^\dagger a_L a_R^\dagger a_R | \psi_\oplus \rangle}{\langle \psi_\oplus | \psi_\oplus \rangle} = \frac{N}{4} (N-1) \left(1 - \frac{z^2}{1 + (\sqrt{1-z^2})^N} \right), \quad (147)$$

$$\langle n_L a_L^\dagger a_R \rangle_\oplus = \langle a_R^\dagger a_L n_L \rangle_\oplus = \langle n_R a_R^\dagger a_L \rangle_\oplus = \langle a_L^\dagger a_R n_R \rangle_\oplus = \frac{(N+1)}{2} \langle a_L^\dagger a_R \rangle_\oplus, \quad (148)$$

$$\langle n_R a_L^\dagger a_R \rangle_\oplus = \langle a_R^\dagger a_L n_R \rangle_\oplus = \langle n_L a_R^\dagger a_L \rangle_\oplus = \langle a_L^\dagger a_R n_L \rangle_\oplus = \frac{(N-1)}{2} \langle a_L^\dagger a_R \rangle_\oplus. \quad (149)$$

From the equation above we can now write the analytical expression for the energy as a function of z

$$E = -\frac{t}{2} N \left(\frac{\sqrt{1-z^2} + (\sqrt{1-z^2})^{N-1}}{1 + (\sqrt{1-z^2})^N} \right) + \frac{U}{4} N (N-1) \left(1 + \frac{z^2}{1 + (\sqrt{1-z^2})^N} \right). \quad (150)$$

If $z = 0$ we recover the energy in the coherent-like state, namely $E = -tN/2 + UN(N-1)/4$, while for $z = 1$ we get the energy in the *NOON* state, $E = UN(N-1)/2$. Eq. (150) should be compared with Eq. (81) (with $\mu = \phi = 0$), called now E_s , the energy calculated considering only a single state, $|\psi_L\rangle$ or $|\psi_R\rangle$, separately. For convenience we report here E_s , the energy of an unbalanced coherent-like state,

$$E_s = -\frac{t}{2}N\sqrt{1-z^2} + \frac{U}{4}N(N-1)(1+z^2). \quad (151)$$

Eq. (151) has a single minimum in $z = 0$ for $U \leq U_c$ and two minima in $z = z_o$ given in Eq. (135), exhibiting a sort of second order phase transition. The concavity at $z = 0$, $d^2E_s/dz^2|_{z=0} = n(t + (N-1)U)/2$, in fact, is negative for $U < U_c$. The concavity of E at $z = 0$, instead, is always negative for any $U < 0$, $d^2E/dz^2|_{z=0} = UN(N-1)/4$. This means that there is always at least one finite minimum, i.e. z_o is finite for any $U < 0$. From Fig. 3 we observe a typical picture of a first order transition, with a jump in the global minimum at some $U_c^* < U_c$, as shown in the left plot of Fig. 4. For $U > U_c^*$ therefore, there is a minimum of the energy E given by

$$z_o \simeq \pm \sqrt{\frac{-2U}{2t + NU}} \quad (152)$$

while for $U < U_c^*$ the minimum is given by Eq. (135). In terms of U_c , Eq. (130), we have, therefore,

$$z_o \simeq \pm \begin{cases} \sqrt{\frac{2U}{(2U_c - U)N}}, & 0 \geq U > U_c^* \\ \sqrt{1 - \left(\frac{U_c}{U}\right)^2}, & U < U_c^* \end{cases} \quad (153)$$

However $U_c^* \rightarrow U_c$ for $N \rightarrow \infty$ (see Fig. 4). More quantitatively, at leading order, we get

$$U_c^* \simeq U_c \left(1 + \frac{1}{\sqrt{2N}}\right). \quad (154)$$

At $U = U_c^*$ there is a small jump in the values of z_o , for N larger than ten, which is given by $\left(1 - \frac{2N}{(\sqrt{2N+1})^2}\right)^{1/2} - \left(\frac{2(\sqrt{2N+1})}{N(\sqrt{2N-1})}\right)^{1/2}$ and which goes to zero as $(\frac{2}{N})^{1/4}$, in the large N limit.

What we have learnt is that, only in the limit of $N \rightarrow \infty$, which implies $E \rightarrow E_s$, the picture of spontaneous symmetry breaking is correct, while for finite N there is always a finite imbalance for any attractive interaction, but always with a null population imbalance.

The number fluctuations on each site, $\sigma_{L,R} = \langle n_{L,R}^2 \rangle_{\textcircled{a}} - \langle n_{L,R} \rangle_{\textcircled{a}}^2$, is given by

$$\sigma = \sigma_L = \sigma_R = \frac{N}{4} + \frac{N(N-1)z^2}{4\left(1 + (\sqrt{1-z^2})^N\right)}, \quad (155)$$

which goes from $\sigma = N/4$ in the coherent-like state ($z = 0$) to $\sigma = N^2/4$ in the *NOON* state ($z = 1$) [41].

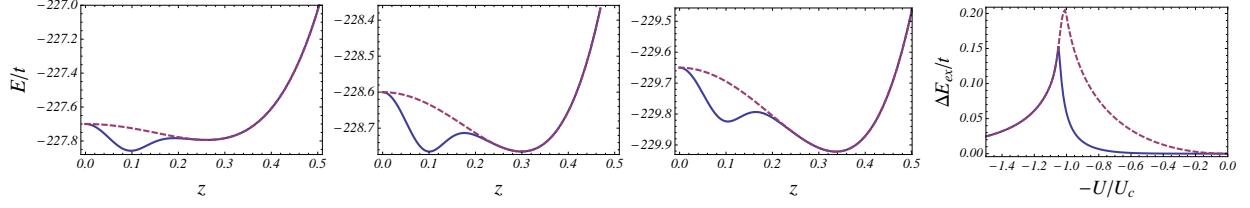


FIG. 3: (Color online) (First three plots) Energy E as a function of z , Eq. (150), for $N = 300$ and $U = x U_c$, with $x = 1.036, 1.048, 1.062$ from left to right. There is a critical interaction $U_c^* < U_c$ at which the global minimum of E jumps from one value of z to the another. The red dashed line is E_s as a function of z , Eq. (151), for the same values of N and U . The energies from exact diagonalization, for those values of interaction, are, respectively, $E_{ex} = -227.97, -228.92, -230.05$ in units of t . (Last plot) Energy differences, between the global minimum of E and the exact ground state energy E_{ex} , i.e. $\Delta E_{ex} = \min(E) - E_{ex}$, (solid blue line) and between the global minimum of E_s and E_{ex} , i.e. $\Delta E_{ex} = \min(E_s) - E_{ex}$, (red dashed line), for $N = 300$. We observe that $\min(E)$ is much better than $\min(E_s)$ for $U > U_c^*$, and deviates from exact ground level mainly for $U \simeq U_c^*$, although, the relative error at that point is still very small, less than 0.07%.

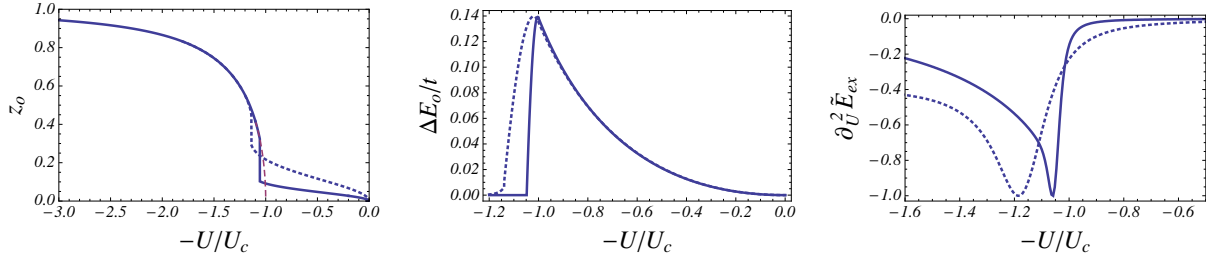


FIG. 4: (Color online) (Left plot) Imbalance z_o , calculated as the global minimum of E given by Eq. (150), as a function of U in units of $(-U_c)$, for $N = 300$ (solid line) and $N = 50$ (dotted line). The red long-dashed line is the plot of z_o given by Eq. (135), i.e. the minimum of E_s given by Eq. (151). We can see that at $U = U_c^* < U_c$ a discontinuity of z_o occurs. (Central plot) Energy difference $\Delta E_o = \min(E_s) - \min(E)$, between the global minimum of E_s and the global minimum of E , as a function of U , for $N = 300$ (solid line) and $N = 50$ (dotted line). ΔE_o is always non-negative, large for $0 > U > U_c^*$ and almost zero for $U \leq U_c^*$. (Right plot) Second derivative of the ground state energy E_{ex} , obtained by exact diagonalization with respect to U , i.e. $\partial^2 E_{ex} / \partial U^2$, as a function of U , for $N = 300$ (solid line) and $N = 50$ (dotted line). The energies E_{ex} have been rescaled for a better comparison: $\tilde{E}_{ex} = E_{ex} / (294.55 t)$, for $N = 300$, and $\tilde{E}_{ex} = E_{ex} / (5.68 t)$, for $N = 50$.

Let us now consider the visibility. Its analytical expression can be read out directly from Eq. (144), therefore

$$\alpha = \left(\frac{\sqrt{1 - z^2} + (\sqrt{1 - z^2})^{N-1}}{1 + (\sqrt{1 - z^2})^N} \right), \quad (156)$$

which is $\alpha = 1$ in the coherent-like state while $\alpha \rightarrow 0$ for $z \rightarrow 1$, namely going towards the *NOON* state.

Finally we calculate the decay rate in the presence of a weak coupling to an external environment, as described before. From Eqs. (144)-(149), we get, for Γ_γ , the following equation, written in terms of the previous quantities

$$\Gamma_\gamma = \sigma|c_L - c_R|^2 + \Gamma_\gamma^h|c_h|^2 + \alpha\frac{N}{2}\text{Re}[(c_L - c_R)c_h^*] \quad (157)$$

and, analogously, $\Gamma_\delta = \sigma|c_L - c_R|^2 + \Gamma_\gamma^h|c_h|^2 - \alpha\frac{N}{2}\text{Re}[(c_L - c_R)c_h^*]$, where σ is given by Eq. (155), α by Eq. (156) and

$$\Gamma_\gamma^h = \frac{N}{2} - \sigma + \frac{N^2}{4}(1 - \alpha^2). \quad (158)$$

For $z = 0$ ($\alpha = 1$, $\sigma = N/4$) we recover the coherent-like result, $\Gamma_\gamma^h = N/4$, while for $z = 1$ ($\alpha = 0$, $\sigma = N^2/4$) we have $\Gamma_\gamma^h = N/2$. For large N , the asymptotic form of Γ_γ^h is

$$\Gamma_\gamma^h \xrightarrow{N \rightarrow \infty} \frac{N}{4}(1 + z^2) \quad (159)$$

while, at finite and large N , Γ_γ^h has a minimum at $z \simeq 1.6/\sqrt{N}$, where $\Gamma_\gamma^h/N \simeq 0.11$, see Fig. 5. However, the important point is that Γ_γ^h does not scale faster than N . In the presence

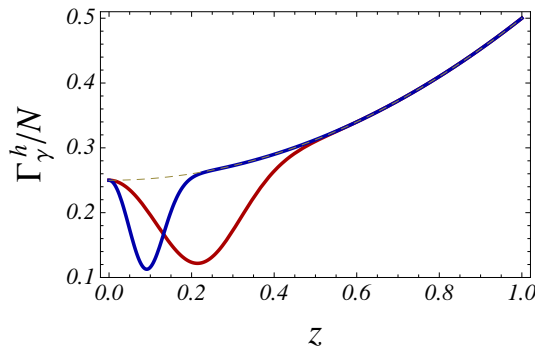


FIG. 5: (Color online) The contribution Γ_γ^h to the decay rate, rescaled by N , as a function of z , for $N = 300$ (solid blue line, with a narrow dip) and $N = 50$ (solid red line, with a broad dip). The dashed line is the limit $N \rightarrow \infty$, Eq. (159).

of a bath coupled differently with the densities located on the two sites ($c_L \neq c_R$), instead, the decay rate Γ_γ , for $U < U_c^*$, scales as N^2 with the number of bosons, since the leading term is driven by the number fluctuations, $\Gamma_\gamma \simeq \sigma|c_L - c_R|^2$, and $\sigma \sim N^2$ for $U < U_c^*$, as one can check from Eq. (155), evaluated at z_o , Eq.(153).

Before we conclude this section a brief explanation is in order. The discontinuity of z_o at U_c^* cannot be directly measured since z_o is not an observable, being not equal to the population imbalance, which is always $\langle n_L \rangle - \langle n_R \rangle = 0$. The small jump in z_o , however

could produce a small discontinuity in the visibility or in the variance of on-site number of bosons as functions of U . By exact diagonalization of H , instead, those quantities do not exhibit any discontinuities. However, the exact results are in a very good agreement with our analytical results away from U_c^* , while, close to U_c^* , those quantities, like the visibility, for instance, obtained by exact diagonalization, are smooth. Nevertheless, their derivatives at U_c^* are large, although not infinite. The analytical expression for the energy is also in perfect agreement with the exact numerical result E_{ex} , see the last plot in Fig. 3 and Fig. 8. It behaves as $\sim UN^2/4 - tN/2$ and $\sim UN^2/2 - tN$ for, respectively, very small and very large interactions. The point of crossover is identified by looking at the minimum of the second derivative of E with respect to U (see the right plot of Fig. 4) which coincides with U_c^* , the point where $(\min(E) - \min(E_s)) \simeq 0$ (compare the right plot and the central plot of Fig. 4). We have checked this result also for different values of N . Therefore, this value of interaction, in the presence of a finite number of bosons, can be promoted as the crossover point, which characterizes the loss of coherence and, as we will see in the next section, is also the point where the quantum entanglement reaches its maximum. Finally, for $U < U_c^*$, as explained in the following paragraph, the cat state becomes extremely fragile under a small offset between the two on-site energies, i.e. $\mu \neq 0$. This fragility is also revealed, as we have seen before, by the decay rate in Eq. (157), when the two sites are coupled differently to a source of noise induced by an external bath, i.e. $c_L \neq c_R$, since, in this case, the instability is driven by the large number fluctuations which goes like N^2 for U more negative than U_c^* .

A. Breakdown of the cat state

The fragility of the Schrödinger cat state can be shown not only by analyzing the decay time $\tau_\gamma = 1/\Gamma_\gamma$, which goes like $1/N^2$, for $U < U_c^*$ and $c_L \neq c_R$, but also by energetic arguments. As one can see from Fig. 4 (central plot) the energy difference ΔE_o between the minimum of E , calculated in the cat state, and the minimum of E_s calculated for a coherent-like state with finite imbalance z , is always positive and becomes almost zero for $U < U_c^*$. Actually, the positions of the global minima of the two energies almost coincide, below that critical interaction, see Fig. 3. However, the energy obtained using the cat state is unaffected by a finite value of the chemical potential difference μ between the two sites, unlike the energy of a coherent state. The latter is modified by an additional term μNz . Therefore, for large N and $U < U_c^*$ an almost infinitesimal value of μ makes the cat state, superposition of two unbalanced coherent-like states, energetically unfavourable with respect to a single coherent-like state. In this case, the number fluctuations and the visibility become simply those in Eqs. (76), (77), or, in terms of z ,

$$\sigma = \frac{N}{4}(1 - z^2), \quad (160)$$

$$\alpha = \sqrt{1 - z^2}. \quad (161)$$

Notice that σ drops the N^2 dependence and becomes linear in the number of bosons. Finally, let us consider the decay rate. If $\mu < 0$ the cat state collapses to $|\psi_L\rangle$ and the decay rate Γ_γ , in terms of z , is given by

$$\Gamma_\gamma = \frac{N}{4} \left\{ |c_L - c_R|^2 (1 - z^2) + |c_h|^2 (1 - z)^2 + 2\sqrt{1 - z^2} \operatorname{Re}[(c_L(1 + z) - c_R(1 - z))c_h^*] \right\}. \quad (162)$$

For Γ_δ one has to interchange c_L with c_R ($c_L \leftrightarrow c_R$) and change the sign of z ($z \rightarrow -z$). If $\mu > 0$, the ground state is, instead, $|\psi_R\rangle$, therefore, the decay rates are the same as before, providing that $z \rightarrow -z$.

X. ENTANGLEMENT FOR $U \leq 0$

A. Entropy

After tracing over one site, for instance, the right one, we get

$$\hat{\rho} = \frac{1}{\langle \psi_{\text{a}} | \psi_{\text{a}} \rangle} \operatorname{Tr}_R (|\psi_{\text{a}}\rangle \langle \psi_{\text{a}}|) = \frac{N!}{\langle \psi_{\text{a}} | \psi_{\text{a}} \rangle} (\hat{\rho}^{LL} + \hat{\rho}^{RR} + \hat{\rho}^{LR} + \rho^{RL}) \quad (163)$$

where $\hat{\rho}^{ss'} = \frac{1}{N!} \operatorname{Tr}_R (|\psi_s\rangle \langle \psi_{s'}|)$, are diagonal matrices with finite elements given by

$$\rho_\ell^o \equiv \rho_\ell^{LL} = \rho_{N-\ell}^{RR} = \binom{N}{\ell} |\xi^>|^{2\ell} |\xi^<|^{2(N-\ell)}, \quad (164)$$

$$\rho_\ell^{LR} = \rho_{N-\ell}^{RL} = \binom{N}{\ell} (\xi^{>*} \xi^<)^{\ell} (\xi^{<*} \xi^>)^{(N-\ell)}, \quad (165)$$

where $|\xi^>|^2 + |\xi^<|^2 = 1$. Eq. (163) is therefore a diagonal matrix, $\rho_{\ell\ell'} = \delta_{\ell\ell'} \rho_\ell$, with

$$\rho_\ell = \frac{1}{2 \left(1 + (\operatorname{Re}[\xi^{>*} \xi^<])^N \right)} \left(\rho_\ell^o + \rho_{N-\ell}^o + \binom{N}{\ell} \operatorname{Re} \left[(\xi^{>*} \xi^<)^N \right] \right). \quad (166)$$

As already said, at the ground state $\phi = 2n\pi$, therefore $\cos \phi = \cos N\phi = 1$, and remembering that $|\xi^{>} \xi^{<}|^2 = (1 \pm z)/2$, we have simply

$$\rho_\ell = \frac{1}{2 \left(1 + (\sqrt{1 - z^2})^N \right)} \left(\rho_\ell^o + \rho_{N-\ell}^o + \frac{1}{2^{N-1}} \binom{N}{\ell} (\sqrt{1 - z^2})^N \right). \quad (167)$$

where ρ_ℓ^o , in terms of z , is given by $\rho_\ell^o = \frac{1}{2^N} \binom{N}{\ell} (1 + z)^\ell (1 - z)^{(N-\ell)}$. It is clear, also by looking at Fig. 6, that the profile of the reduced density matrix has a bimodal shape, peaked at the values $N(1 + z)/2$ and $N(1 - z)/2$, with an additional interference term. When z is

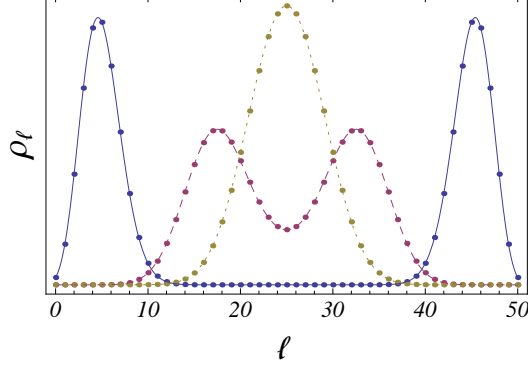


FIG. 6: (Color online) Reduced density matrix for $N = 50$ and $z = 0.1$ (yellow dotted line), $z = 0.3$ (red dashed line), $z = 0.8$ (blue solid line). The lines are guides for the eye.

small the two peaks merge together, while for z close to 1 the two peaks are far apart. For $z = 0$, in fact, we recover the coherent-like reduced density matrix

$$\rho_\ell = \frac{1}{2^N} \binom{N}{\ell}, \quad (168)$$

while for $z = 1$, namely in the *NOON* state, we have

$$\rho_\ell = \frac{1}{2} (\delta_{\ell,0} + \delta_{\ell,N}). \quad (169)$$

Now we can calculate the entanglement von Neumann entropy, whose expression is here reported,

$$S = - \sum_{\ell=0}^N \rho_\ell \log_2 \rho_\ell. \quad (170)$$

For $z = 0$ and for large N the reduced density matrix approaches a gaussian distribution, $\rho_\ell \simeq \frac{1}{\sqrt{\pi N/2}} \exp\left[-\frac{(\ell-N/2)^2}{N/2}\right]$, therefore, the asymptotic behavior for the entanglement entropy in the coherent-like state is given by Eq. (113), namely

$$S_o = \frac{1}{2} \log_2 \left(\frac{\pi e}{2} N \right). \quad (171)$$

For $z = 1$, in the *NOON* state, instead, since the reduce density matrix is given by Eq. (169), and then the entropy is simply

$$S_1 = 1. \quad (172)$$

For finite z , in the large N limit, we can approximate the reduced density matrix as $\rho_\ell \simeq \frac{1}{2}(\rho_\ell^o + \rho_{N-\ell}^o)$, i.e. as the sum of two gaussians, therefore, if z is large enough that the two gaussians are well separated, the entropy has the following asymptotic form

$$S_z \simeq \frac{1}{2} \log_2 (2\pi e N (1 - z^2)), \quad (173)$$

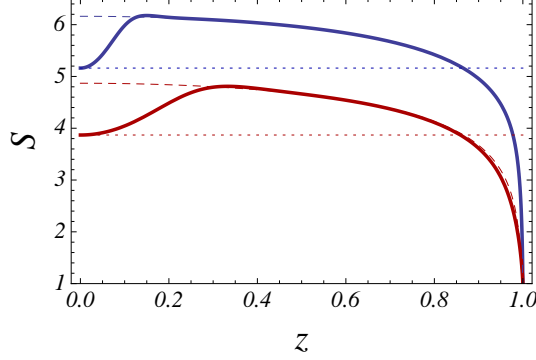


FIG. 7: (Color online) Entanglement entropy, S , in the cat state, as a function of z , for $N = 300$ (upper solid line) and $N = 50$ (lower solid line). The dashed lines are the asymptotic behaviors given by Eq. (173), for $N = 300$ (upper dashed line) and $N = 50$ (lower dashed line), which match the exact entropy for $z > 2.6/\sqrt{N}$. The straight dotted lines are the values of S for $z = 0$, given by Eq. (171), i.e. S_o , the entropy of the coherent state, for $N = 300$ (upper dotted line) and $N = 50$ (lower dotted line).

where, of course, $z^2 < 1 - 2/\pi eN$ in order not to go below the *NOON* entropy or even to diverge. Approaching $z \rightarrow 0$ the two separated gaussians of the reduced density matrix, see Fig. 6, which gives the entropy in Eq. (173), start to see each other when the distance between the two peaks, which is Nz , becomes smaller than a certain number, n_σ , of standard deviations, $\sigma_g = \sqrt{N(1 - z^2)}/4$, of each gaussian. Namely, the entropy reaches its maximum and then starts to decrease approaching $z = 0$, when z fulfils

$$Nz \simeq 2\sigma_g n_\sigma, \quad (174)$$

whose solution is given by

$$z_{S_{max}} \simeq \frac{n_\sigma}{\sqrt{n_\sigma^2 + N}}. \quad (175)$$

From Fig. 7, and further checks, in fact, we have found that the number of standard deviations, consistent with such a description, is $n_\sigma \approx 2.6$, therefore the maximum value for the entropy is reached at $z_{S_{max}} \approx 2.6/\sqrt{N}$, corresponding to having a distance between the two peaks of the reduced density matrix approximately equal to five sigmas. If z were given by Eq. (135), the entropy would reach its maximum at $U_{S_{max}} \simeq U_c \sqrt{\frac{N+n_\sigma^2}{N}} \simeq U_c \left(1 + \frac{n_\sigma^2}{2N}\right)$. However, since $z_o|_{U_c^* - \varepsilon} < z_{S_{max}} < z_o|_{U_c^* + \varepsilon}$, then the maximum entropy occurs at

$$U_{S_{max}} = U_c^*, \quad (176)$$

where U_c^* is given by Eq. (154). For large N , $z_{S_{max}}$ goes to zero, and, as a result, the asymptotic value of the maximum entropy can be written simply substituting z with 0 in Eq. (173), getting

$$S_{max} \simeq \frac{1}{2} \log_2(2\pi eN) = S_o + 1, \quad (177)$$

which does not depend on the interaction strength. In conclusion, the entropy grows up to 1 above its value at $U = 0$, Eq. (171), within a short range of interaction close to the value U_c^* , Eq. (176). Strikingly, from Eq. (173), we have that the entropy exceeds its coherent value ($S > S_o$) for $0 < z \lesssim \sqrt{3}/2$. In terms of the interaction, this means that

$$S > S_o, \text{ for } 2U_c \lesssim U < 0. \quad (178)$$

B. Fisher information

From the definition of Fisher information, Eq. (124), and after verifying that

$$\langle n_L n_R \rangle_{\textcircled{a}} - \langle n_L \rangle_{\textcircled{a}} \langle n_R \rangle_{\textcircled{a}} = -\sigma \quad (179)$$

where σ is given by Eq. (155), we find the following remarkable exact result

$$F = \frac{4\sigma}{N^2}, \quad (180)$$

valid along all the attractive regime, from $z = 0$ ($U = 0$, coherent-like state), where $\sigma = N/4$ and $F = 1/N$, to $z = 1$ ($U \rightarrow -\infty$, *NOON* state), where $\sigma = N^2/4$ and $F = 1$. Even if the system collapses into an unbalanced coherent-like state, Eq. (180) is still valid, providing that σ is given by Eq. (160). Surprisingly, Eq. (180) is the same relation as that obtained also for repulsive interaction, Eq. (128).

XI. SUMMARY OF MAIN RESULTS WITH PLOTS

In this section we show some plots of several quantities: energy (Fig. 8), coherence visibility (Fig. 9), Fisher information (Fig. 10), and entanglement entropy (Fig. 11), all as functions of the interaction strength, both in the attractive and repulsive regimes. We used $N = 50$ in order to show features visible only for not too large number of particles.

XII. CONCLUSIONS

We have studied, in the repulsive regime, the interpolation from a spatial separated Fock state, ground state in the limit of strong repulsive interaction of the Bose-Hubbard Hamiltonian, to a delocalized coherent state, ground state for free bosons. We have used as many-body wavefunction a simplified permanent state which allows us to write all the physical quantities we are interested in in terms of polynomials of the single particle overlap parameter which can be determined variationally. Although not exact, our single particle approach provides a quite transparent and intuitive description of the crossover between the two exact limits. We have calculated the energy, the charge fluctuations, the decay rate, the coherence visibility, the entanglement entropy and the Fisher information with such a

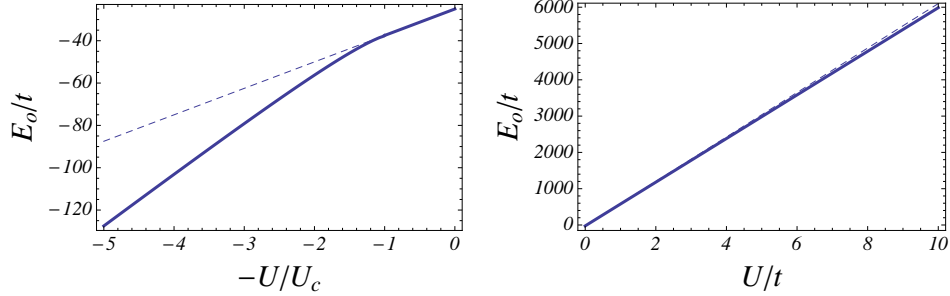


FIG. 8: (Color online) Ground state energy $E_o = \min(E)$ as a function of U for $N = 50$, for attractive (left plot) and repulsive (right plot) interactions. Left plot (attractive interaction): the energy is described by Eq. (150) at z_o given by Eq. (153). Right plot (repulsive interaction): the energy is described by Eq. (103). In both the plots, the dashed line is the coherent energy, $E_C = -t/2 + UN(N-1)/4$, showing that a finite imbalance lowers the ground state energy. The ground state energy obtained by exact diagonalization, E_{ex} , coincides, on the scale of the plots, with the analytical result E_o (solid line), in both the regimes.

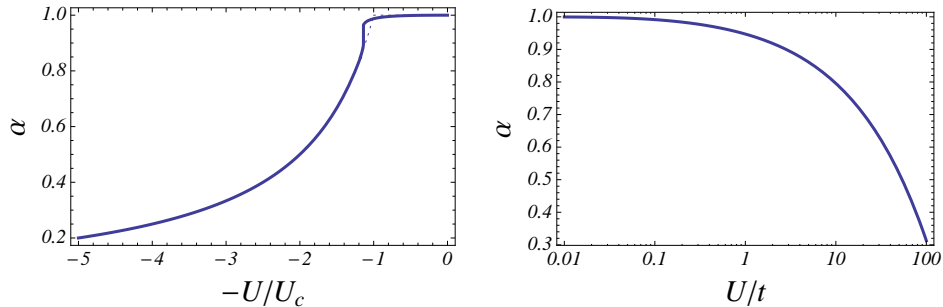


FIG. 9: (Color online) Visibility α as a function of U for $N = 50$, for attractive (left plot) and repulsive (right plot) interactions. Left plot (attractive interaction): the visibility as in Eq. (156), calculated at z_o given by Eq. (153). The dotted line is the limit $N \rightarrow \infty$. Right plot (repulsive interaction): the visibility described by Eq. (104).

trial wavefunction. We have derived a non-perturbative, simple analytical expression for the ground state energy in the large N limit. We have shown that the charge fluctuation, null in the Fock limit while proportional to N for zero interaction, in the presence of finite interaction scales as $N^{1/2}$ with the number of bosons. Moreover we have shown that the decay rate, in the presence of a weak coupling with an external environment, scales as $N^{3/2}$ in the intermediate case, i.e. finite U , and that it is proportional to the inverse of the Fisher information. In this regard, the overlap of single bosons can be considered as the key parameter which contains the quantum information. Moreover we have shown that, for $U \ll N$, the Fisher information F and the on-site number fluctuations expressed by the variance σ are related by the equation $F = 4\sigma/N^2$. In the attractive regime we have

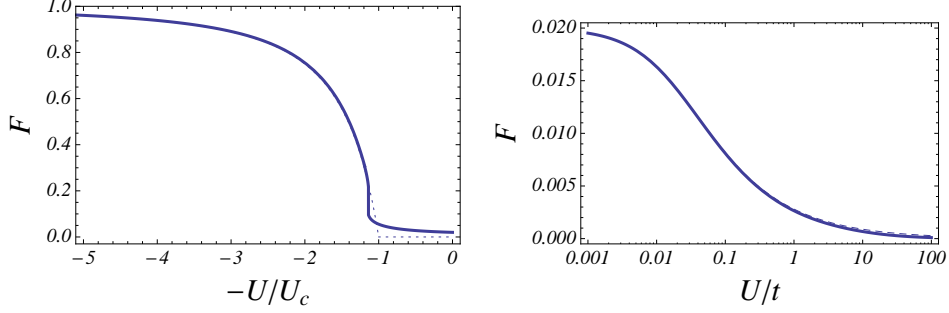


FIG. 10: (Color online) Fisher information F as a function of U , for $N = 50$, for attractive (left plot) and repulsive (right plot) interactions. The Fisher information is described by $F = 4\sigma/N^2$ where σ is the variance of the number of particles. Left plot (attractive interaction): σ is given by Eq. (155), calculated at z_o in Eq. (153). The dotted line is the limit $N \rightarrow \infty$. Right plot (repulsive interaction): F given by Eq. (123), calculated from full correlators, Eqs. (30), (32), with parametrizations Eq. (94), (95), at $\omega = \omega_o$, Eq. (99). The dashed line, which almost coincides with the solid one, is simply given by Eq. (126) at ω_o .

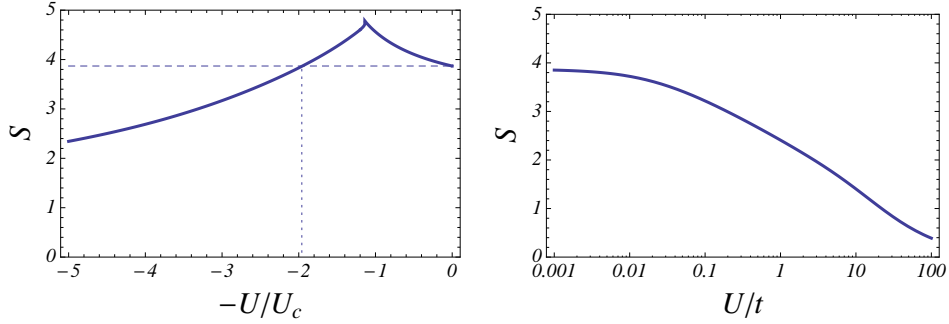


FIG. 11: (Color online) Entanglement entropy S as a function of U , for $N = 50$, for attractive (left plot) and repulsive (right plot) interactions. Left plot (attractive interaction): S is given by Eq. (170), with ρ_ℓ obtained from Eq. (167), calculated at z_o in Eq. (153). The dashed line corresponds to S_o , Eq. (171). S exceeds S_o for $2U_c \lesssim U < 0$. Right plot (repulsive interaction): entropy calculated through Eqs. (107), (108), with $n = k = N/2$ and Eqs. (94), (95), at ω_o , Eq. (99).

calculated again the energy, the variance of bosonic numbers σ , the decay rate, the visibility, the Fisher information and the entanglement entropy by using a symmetric superposition of imbalanced coherent-like states, namely a Schrödinger cat state. We have shown that this state, in the absence of a local offset between the two on-site energies, has always a lower energy with respect to a single coherent-like state which usually is supposed to describe well the low interaction regime. As a result, the symmetry breaking for finite number of bosons does not occur, and the corresponding critical interaction U_c , shifted toward more negative U , i.e. $U_c^* \simeq U_c(1 + \frac{1}{\sqrt{2N}})$, is actually a crossover point separating two different regimes, the

coherent regime and the incoherent one; in the latter regime the cat state becomes extremely fragile. In the presence of an external bath, if the environment is coupled differently to the two local densities the relaxation time is very short, inversely proportional to the number fluctuations which go like N^2 for $U < U_c^*$. Remarkably, we have found that the equation for the Fisher information, derived in the repulsive regime, i.e. $F = 4\sigma/N^2$, is exactly valid also for the whole range of negative interactions. Finally, we have calculated the entanglement entropy and found that, close to the crossover point, U_c^* , the entropy reaches its maximum value, which, in the large N limit, is equal to the entropy at $U = 0$, increased by one (notice that 1 is the entropy in the *NOON* state). Another important and final result, valid for large N , is that the entanglement entropy exceeds its coherent value (at $U = 0$) for $2U_c \lesssim U < 0$.

Acknowledgments

I thank F. Benatti, R. Floreanini, M. Fabrizio, G. Mazzarella, L. Salasnich, F. Toigo and A. Trombettoni for useful discussions and acknowledge financial support by the Department of Physics -Miramare-, University of Trieste, during the first stage of the work, and hospitality by SISSA, Trieste. I dedicate this work to Sasha Gogolin, a dear friend and great scientist.

-
- [1] A. Imamoglu, M. Lewenstein, and L. You, Phys. Rev. Lett. **78**, 2511 (1997).
 - [2] Y. Castin and J. Dalibard, Phys. Rev. A **55**, 4330 (1997).
 - [3] R. Graham, T. Wong, M.J. Collett, S.M. Tan, and D.F. Walls, Phys. Rev. A **57**, 493 (1998).
 - [4] J. I. Cirac, M. Lewenstein, K. Molmer, and P. Zoller, Phys. Rev. A **57**, 1208 (1998).
 - [5] M.J. Steel and M.J. Collett, Phys. Rev. A **57**, 2920 (1998).
 - [6] J. Javanainen, M.Y. Ivanov, Phys. Rev. A **60** 2351 (1999).
 - [7] D. Jaksch, C. Bruder, J.I. Cirac, C.W. Gardiner, P. Zoller, Phys. Rev. Lett. **81** 3108 (1998).
 - [8] M. Lewenstein, A. Sanpera, V. Ahufinger, B. Damski, A. Sen De, U. Sen, Adv. Phys. **56** 243 (2007).
 - [9] J. R. Anglin, P. Drummond, A. Smerzi, Phys. Rev. A **64**, 063605 (2001).
 - [10] F. Dalfovo, S. Giorgini, L. P. Pitaevskii, S. Stringari, Rev. Mod. Phys. **71**, 463 (1999).
 - [11] R. Alicki, F. Benatti, R. Floreanini, Phys. Lett. A, **372** 1968 (2008).
 - [12] F. Benatti, R. Floreanini, J. Realpe-Gómez, J. Phys. A: Math. Gen. **41** 235304 (2008).
 - [13] D.V. Averin, T. Bergeman, P.R. Hosur, and C. Bruder, Phys. Rev. A **78**, 031601(R) (2008).
 - [14] A. Wagner, C. Bruder, E. Demler, Phys. Rev. A **84**, 063636 (2011).
 - [15] J. Links, H.-Q. Zhou, Lett. Math. Phys **60** (2002) 275-282.
 - [16] P. Buonsante, R. Burioni, E. Vescovi, A. Vezzani, arXiv:1112.3816.

- [17] F. S. Cataliotti, S. Burger, C. Fort, P. Maddaloni, F. Minardi, A. Trombettoni, A. Smerzi and M. Inguscio, *Science* **293**, 843 (2001).
- [18] Y. Shin, M. Saba, T. A. Pasquini, W. Ketterle, D. E. Pritchard, and A. E. Leanhardt, *Phys. Rev. Lett.* **92**, 050405 (2004).
- [19] M. Albiez, R. Gati, J. Fölling, S. Hunsmann, M. Cristiani, and M. K. Oberthaler, *Phys. Rev. Lett.* **95**, 010402 (2005).
- [20] S. Levy, E. Lahoud, I. Shomroni, J. Steinhauer, *Nature (London)* **499**, 579 (2007).
- [21] J. Javanainen, *Phys. Rev. Lett.* **57**, 3164 (1986).
- [22] G. J. Milburn, J. Corney, E. M. Wright, and D. F. Walls, *Phys. Rev. A* **55**, 4318 (1997).
- [23] A. Smerzi, S. Fantoni, S. Giovanazzi, S. R. Shenoy, *Phys. Rev. Lett.* **79** 4950 (1997).
- [24] S. Raghavan, A. Smerzi, S. Fantoni, S. R. Shenoy, *Phys. Rev. A* **59** 620 (1999).
- [25] L. Salasnich, B. A. Malomed, and F. Toigo, *Phys. Rev. A* **81**, 045603 (2010).
- [26] D. A. R. Dalvit, J. Dziarmaga, and W. H. Zurek, *Phys. Rev. A* **62**, 013607 (2000).
- [27] Y. P. Huang and M. G. Moore, *Phys. Rev. A* **73**, 023606 (2006).
- [28] G. Mazzaella, L. Salasnich, A. Parola, F. Toigo, *Phys. Rev. A* **83** 053607 (2011).
- [29] L. Amico, R. Fazio, A. Osterloh, V. Vedral, *Rev. Mod. Phys.* **80**, 517 (2008).
- [30] M. Haque, O. S. Zozulya, and K. Schoutens, *J. Phys. A: Math. Theor.* **42**, 504012 (2009).
- [31] L. Dell'Anna, M. Fabrizio, *J. Stat. Mech.* (2011) P08004.
- [32] F. Benatti, R. Floreanini, *Int. J. Mod. Phys. B* **19** 3063 (2005).
- [33] V. Gorini, A. Kossakowski, *J. Math. Phys.* **17** 1298 (1976).
- [34] L. Pitaevskii and S. Stringari, *Phys. Rev. Lett.* **83**, 4237 (1999).
- [35] L. Pitaevskii and S. Stringari, *Phys. Rev. Lett.* **87**, 180402 (2001).
- [36] G. Ferrini, A. Minguzzi, and F. W. J. Hekking, *Phys. Rev. A* **78**, 023606(R) (2008).
- [37] L. Radzihovsky, V. Gurarie, *Phys. Rev. A* **81** 063609 (2010).
- [38] W.K. Wootters, *Phys. Rev. D.* **23**, 357 (1981).
- [39] L. Pezzè and A. Smerzi, *Phys. Rev. Lett.* **102**, 100401 (2009).
- [40] B. Gertjerenken, S. Arlinghaus, N. Teichmann, C. Weiss *Phys. Rev. A* **82**, 023620 (2010).
- [41] K. Sakmann, A.I. Streltsov, O.E. Alon, L.S. Cederbaum, *Phys. Rev. A* **84**, 053622 (2011).